frontiers | Frontiers in Earth Science

TYPE Original Research
PUBLISHED 07 June 2024
DOI 10.3389/feart.2024.1403411

Check for updates

OPEN ACCESS

EDITED BY
Wen Nie,
Jiangxi University of Science and Technology, China

REVIEWED BY
Ionut Cristi Nicu,
Norwegian Institute for Cultural Heritage Research, Norway
Xuexue Su,
Anhui University of Science and Technology, China
Kai Kang,
Jiangnan University, China

*CORRESPONDENCE
Cristian Constantin Stoleriu,
cristoan@yahoo.com

RECEIVED 19 March 2024
ACCEPTED 22 May 2024
PUBLISHED 07 June 2024

CITATION
Mihu-Pintilie A, Stoleriu CC and Urzică A (2024), UAV and field survey investigation of a landslide triggered debris flow and dam formation in Eastern Carpathians.
Front. Earth Sci. 12:1403411.
doi: 10.3389/feart.2024.1403411

COPYRIGHT
© 2024 Mihu-Pintilie, Stoleriu and Urzică. This is an open-access article distributed under the terms of the Creative Commons Attribution License (CC BY). The use, distribution or reproduction in other forums is permitted, provided the original author(s) and the copyright owner(s) are credited and that the original publication in this journal is cited, in accordance with accepted academic practice. No use, distribution or reproduction is permitted which does not comply with these terms.

UAV and field survey investigation of a landslide triggered debris flow and dam formation in Eastern Carpathians

Alin Mihu-Pintilie[1], Cristian Constantin Stoleriu[2]* and Andrei Urzică[2,3]

[1]Institute of Interdisciplinary Research, Department of Exact and Natural Sciences, University "Alexandru Ioan Cuza" of Iași, Iași, Romania, [2]Faculty of Geography and Geology, Department of Geography, University "Alexandru Ioan Cuza" of Iași, Iași, Romania, [3]Research Center with Integrated Techniques for Atmospheric Aerosol Investigation in Romania (RECENT AIR), Laboratory of Interdisciplinary Research of Mountain Environment, Ion Gugiuman, Rarău Station for Research and Students Fellowships, Câmpulung-Moldovenesc, Suceava, Romania

In the May–August period of 2010, major heavy rains impacted the Eastern Carpathians (Northeastern Romania), leading to flash floods and triggering numerous landslides. The extreme weather conditions caused damage to the road network, extensive forest destruction, and lead to formation of impounded lakes. One of the hardest-hit areas was the mountain tributaries catchments of the Bistrița watershed. Particularly, the most significant landslide-triggered debris flow event occurred in the upper Iapa valley (Neamț County). The landslide process started near the top of the Drumul Chinezilor ridge in the Goșmanu-Geamăna Massif (Tarcău Mountains), at an elevation of 875 m a.s.l., and the flow-slide fan obstructed a 300-m section of the Iapa watercourse at 615 m a.s.l. This study compiles the climatic, anthropogenic, geological, and geomorphological evidence gathered during the field investigation in the October 2023 and utilizes Unmanned Aerial Vehicle (UAV) data collected to reconstruct the occurred debris flow-slide event. Additionally, it explores considerations regarding the reactivation of landslide processes, dam stability, and the future evolution of the impounded lake (Făgețel Lake: water surface area of 9,500 m^2; maximum depth 10 m). Furthermore, the lessons learned and future actions required to prevent further mass movement associated with debris flow-slide processes in prone areas of the Eastern Carpathians are discussed.

KEYWORDS

weather-induced landslides, landslide-triggered debris flow (LDF), dam formation, impounded lake, UAV, Eastern Carpathians

1 Introduction

In recent decades, the escalating frequency of extreme rainfall as a consequence of ongoing climate change has been linked to an observed increase in the occurrence and magnitude of various types of geomorphological (e.g., erosion, landslides) and hydrological (e.g., floods, flash floods) hazards (Neumayer and Barthel, 2011; Diffenbaugh and Field, 2013; Gariano and Guzzetti, 2016). This trend also includes the catastrophic events triggered by landslides leading to debris flows (Yang et al., 2020; Yang et al., 2023). In this context, if landslides can be triggered by various climatic,

geomorphological, seismic, or anthropogenic factors (Cruden and Varnes, 1996; Hungr et al., 2014), debris flows occur only when a mixture of earth material, water, and air rapidly surges down steep drainage paths (over 25°), with their primary trigger being high-intensity rainfall (Hürlimann et al., 2019; Scheip and Wegmann, 2022; De Falco et al., 2023). Therefore, in this specific weather and geomorphic conditions, the combination of landslides and debris flow (debris flow-slide) in the same event poses a higher threat to human life and infrastructure, owing to their sudden occurrence, high mobility, volume, impact energy, and extensive run-out distance (Gariano and Guzzetti, 2016). However, whether landslides and debris flows occur separately or in combination, triggering each other (Iverson et al., 1997; Sassa and Wang, 2005), they are responsible for thousands of casualties and economic losses every year (Costa and Schuster, 1988; Kahn, 2005; Petley, 2012).

Generally, the term debris flow is associated with a wide variety of hydrogeomorphic processes and phenomena (e.g., debris torrents, debris slides, mudflows, debris floods, mudslides), usually specific to steep slopes (e.g., mountains, cliffs) frequently impacted by extreme weather conditions (Santangelo et al., 2021; Ortiz-Giraldo et al., 2023). In this context, the interactions between debris flows induced by heavy rainfall and hydrographic network are topics of great relevance for understanding slope evolution, as well as the implications for flood hazards within exposed watersheds (Korup, 2005; Chien-Yuan et al., 2008; Cao et al., 2011a; Cao et al., 2011b; Marchi, 2017). However, the main issue with these types of hydrogeomorphic processes is their relative difficulty in prediction and monitoring due to their rapid manifestation. Therefore, the utilization of remote sensing techniques and optical imagery derived from Unmanned Aerial Vehicles (UAV) surveys has become a very useful tools for observing and monitoring the areas affected by landslides, debris flow and rockfalls (Blanch et al., 2024). Furthermore, recent advancements in GIS algorithms, coupled with the ability to obtain images from UAVs (Colomina and Molina, 2014), are driving significant advances in various geoscience applications such as automatically calculating the volume of material eroded in gullies (Neugirg et al., 2016), multitemporal monitoring of landslides (Blanch et al., 2021; Fang et al., 2024) or shoreline transformation rates (Yermolaev et al., 2021), and flood monitoring using aerial images and videos (Eltner et al., 2021).

In the Carpathians, as is other mountainous regions of Europe (Tiranti et al., 2018; Frank et al., 2019; De Falco et al., 2023; Tichavský et al., 2023), debris flow is one of the most frequent processes threatening local communities (Ilinca, 2014; Vădean et al., 2015; Mihu-Pintilie et al., 2016; Pop et al., 2019). This hazard is due to their high mobility induced by rainfall, which particularly affects flysch deposits and can cause damage not only within and adjacent to the flow-slide sector, but also in the depositional area (Santo et al., 2018). Furthermore, in some specific morpho-hydrological conditions, debris fans can temporarily block valleys, leading to the formation of dams and impounded lakes (Costa and Schuster, 1988; Evans, 2006; Fan et al., 2020). In these cases, the risk of dam failure exposes downstream communities and infrastructure to flash floods (Costa and Schuster, 1988; Dai et al., 2005; Cao et al., 2011a; 2011b), mudflows (Sepúlveda and Padilla, 2008; Tannant and Skermer, 2013), and other destructive events associated with lateral erosion (Zhao et al., 2022). Consequently, detailed hazard assessments are needed, firstly to the flow-slide sector and depositional area to protect people and infrastructure from future events, and secondly for dam stability to better manage the associated risks.

In the flysch belt of the Eastern Carpathians (Romania) (Belayouni et al., 2009; Miclauș et al., 2009), where the study site is located (Figure 1A) most landslides and landslide triggered debris flow occur in remote locations and usually do not pose a significant hazard (Mihu-Pintilie et al., 2014b; Mihu-Pintilie et al., 2016) (Figure 1B). However, some debris flow-slide events have impacted road infrastructure located at the base of slopes and caused extensive forest destruction, with a moderate impact on the local economy (Pop et al., 2017). In some cases, the debris fan deposits lead to the formation of temporary or, very rarely, long-term water accumulation behind the dams (Mihu-Pintilie, 2018a). One of the most recent landslide and rainfall-induced debris flow events occurred in the summer of 2010, in the upper Iapa valley, a right tributary of the Bistrița River (Figure 1C). Initially starting as a landslide process near the top of the Goșmanu-Geamăna Massif (Tarcău Mountains) at an elevation of 875 m a.s.l., the debris flow deposits obstructed a 300-m section of the Iapa watercourse at 615 m a.s.l., forming a 10 m depth lake, currently known as Făgețel Lake (Figure 1D). The main trigger was the heavy rains that impacted the entire region during the May-July period of 2010 (Romanescu et al., 2017; Romanescu et al., 2018a), but the high density of the forest paths and extensive deforestation in the Limpedea logging area have also a significant contribution in geomorphological process that affect the southern slope of the Drumul Chinezilor ridge. However, the most interesting aspect related to the Iapa landslide triggered debris flow (Iapa LDF) is that of more than 20 large landslide dams formed due to extreme hydro-climate conditions in the Carpathian Mountains, investigated and reported in various studies (Năstase, 1949; Ciornei, 1959; Tövissi, 1964; Pop, 1970; Decei, 1981; Ichim and Rădoane, 1996; Ilinca and Gheuca, 2011; Șerban et al., 2012; Romanescu et al., 2013; Mihu-Pintilie, 2014a; Mihu-Pintilie et al., 2014b; Stoleriu et al., 2014; Mihu-Pintilie et al., 2016; Lesenciuc et al., 2017; Mihu-Pintilie et al., 2018a; Romanescu et al., 2018b), the Iapa LDF event is the singular one in the Eastern Carpathians that has formed a long-term lake (more than 10 years) due to a debris flow-slide dam (Table 1).

In this work, the rainfall data collected during the May–August period of 2010 are reported for the first time in order to describe the Iapa LDF occurrence scenario and Făgețel Lake formation. This case study is of interest to the international community because these hazardous phenomena occur in many places on Earth where debris materials and loose soils cover steep bedrocks, posing a threat to the communities living in the affected areas or along the dammed valleys. The paper includes descriptions of rainfall data, the anthropogenic impact on destabilized slopes, and the geological, geomorphological and hydrological setting. Additionally, it focuses on the UAV methodology employed in the post-event survey to produce the accurate maps of the entire affected area. Finally, in the concluding remarks section, the lessons learned and future actions needed to prevent the further reactivation of the Iapa LDF are discussed.

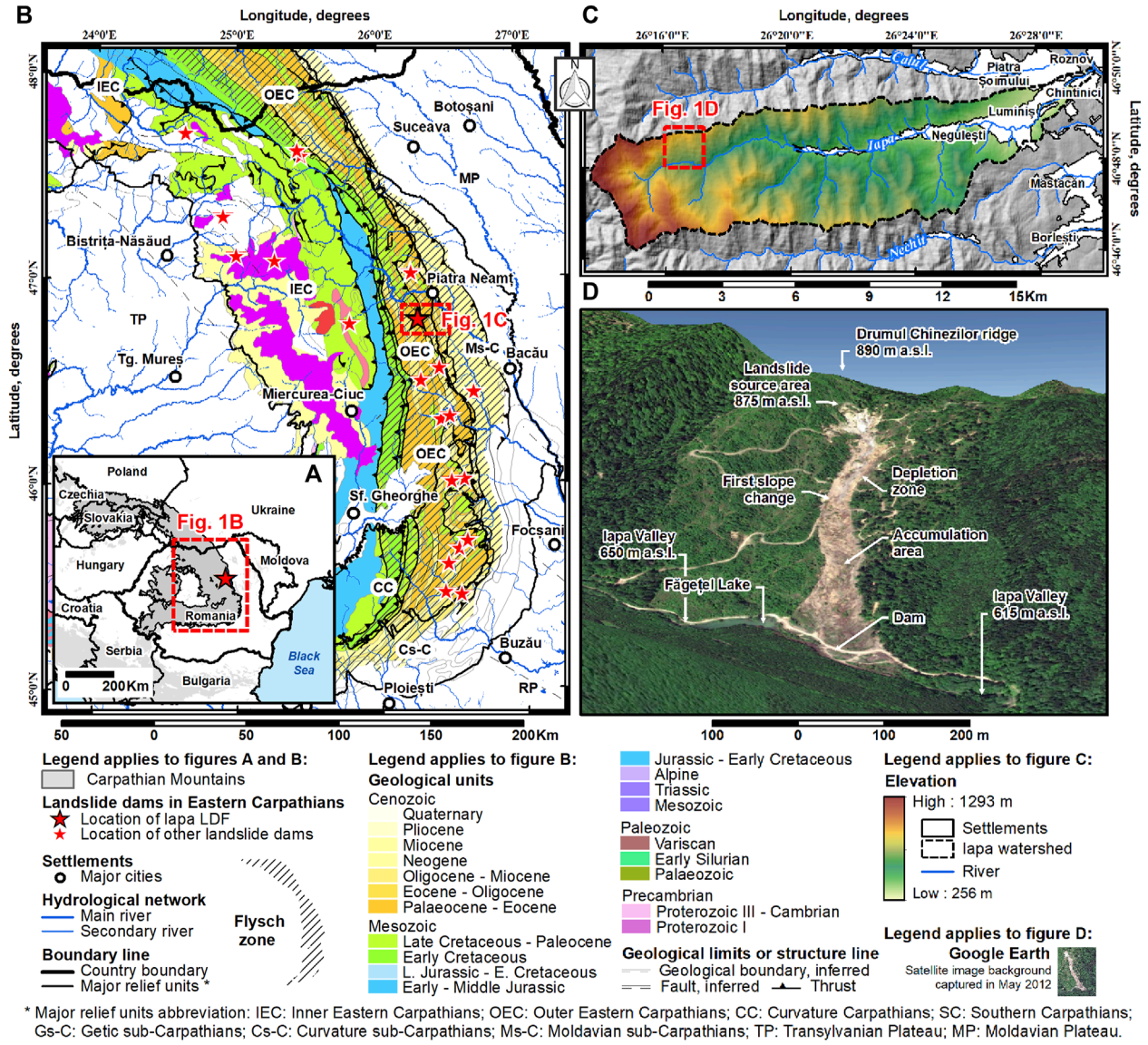

FIGURE 1
Geographic location of the Iapa LDF. **(A)** and other landslide dams (see Table 1), **(B)** in the flysch zone of the Eastern Carpathians. In **(C)**, the UAV mapped area is highlighted in the upper Iapa watershed, represented in **(D)** as 3D image.

2 Study area and regional setting

The investigated Iapa LDF, occurred in the upper part of the Iapa watershed (46°48′34″N/26°16′19″E) which drains the northeastern side of the Goșmanu-Geamăna Massif (eastern Tarcău Mountains), part of the central group of the Eastern Carpathians. With a total length of 25.3 km, the Iapa River flows from west to east and serves as a right-side tributary of the Bistrița River, joining it near Roznov (Neamț County). Downstream of the Iapa LDF dam, four settlements are potentially at risk in the event of a dam failure: Negulești (639 inhabitants), Luminiș (2,295 inhabitants), Piatra-Șoimului (4,015 inhabitants), and Chintinici (823 inhabitants) (Figure 1C). In the forthcoming subsections, we will delve into the geological, climatic, hydrological, and anthropogenic factors that significantly contributed to the formation of the LDF dam and Lake Făgețel (Figure 2).

2.1 Geological background

The upper Iapa watershed is located within the Bistrița Half-window (Outer Carpathians Flysch Zone), where the Tarcău and Vrancea Nappe's (Outer Moldavides), are exposed. Dominating the landscape are vertical or reversed anticlines and synclines, which took shape during the Upper Cretaceous to Lower Miocene period. Overall, the geological formations exhibit a distinct north-south orientation, with faulted flanks characterized by a vertical or reversed configuration (Brustur et al., 2019).

TABLE 1 Examples of rainfall-induced landslide dams and lake formations in the Eastern Carpathians.

Lake name	Mountain unit	River	Location (UTM)	Landslide age	Landslide type	Dam failure	Supporting references
Făgeţel L.	Goşmanu Mts.	Iapa	5245552/1360319	2010	Rock slide and debris flow	Did not fail	Mihu-Pintilie (2018a), Romanescu et al. (2018b)
Palcău L.	Vrancea Mts.	Palcău	5129688/1402860	2008	Rock slide	Failed	Mihu-Pintilie (2018a)
Topliţa L.	Goşmanu Mts.	Topliţa	5220820/1375442	2005	Rock slide	Did not fail	Mihu-Pintilie (2018a)
Lacul cu Boglari	Berzunţi Mts.	Strâmba	5210377/1395619	2002	Slide	Partial fail	Mihu-Pintilie (2018a)
Agăş L.	Tarcău Mts.	Muncel	5212655/1366174	2000	Rock slide	Partial fail	Mihu-Pintilie (2018a), Romanescu et al., (2018b)
Cuejdel L.	Stânişoarei Mts.	Cuejdel	5270636/1275295	1991	Rock slide	Did not fail	Ichim and Rădoane (1996), Mihu-Pintilie (2018a), Mihu-Pintilie (2018b), Mihu-Pintilie et al. (2014a), Mihu-Pintilie et al. (2014b), Mihu-Pintilie et al. (2016), Stoleriu et al. (2014)
Constellation L.	Stânişoarei Mts.	Cuejdel	5269954/1353255	1991	Rock slide	Did not fail	Ichim and Rădoane (1996), Mihu-Pintilie (2018b), Mihu-Pintilie et al. (2016)
Lacul fără nume	Vrancea Mts.	Zăbala	5124514/1398789	1977	Rock slide	Did not fail	Mihu-Pintilie (2018a), Romanescu et al. (2018b)
Old Green L.	Vrancea Mts	Lepşa	5160653/1389939	1971	Rock slide	Failed	Mihu-Pintilie (2018a), Romanescu et al. (2018b), Tövissi (1964)
Betiş (Novăţ) L.	Maramureş Mts.	Novăţ	5329417/1221978	1957	Rock slide	Failed	Ciornei (1959), Mihu-Pintilie (2018a), Romanescu et al. (2018b)
Green L.	Vrancea Mts.	Chiua Mica	5162508/1396776	1940	Rock slide	Failed	Decei (1981), Mihu-Pintilie (2018a), Romanescu et al. (2018b)

(Continued on the following page)

10.3389/feart.2024.1403411

TABLE 1 (*Continued*) Examples of rainfall-induced landslide dams and lake formations in the Eastern Carpathians.

Lake name	Mountain unit	River	Location (UTM)	Landslide age	Landslide type	Dam failure	Supporting references
Bolătău L.	Nemira Mts.	Izvorul Negru	5193224/1379992	1883	Rock slide	Failed	Nastase (1949), Mihu-Pintilie (2018a), Romanescu et al. (2018b)
Red L.	Hășmaș Mts.	Bicaz	5238159/1323933	1837	Rock slide	Did not fail	Mihu-Pintilie (2018a), Romanescu et al. (2013), Stoleriu et al. (2014)
Iezerul Sadovei	Obcina Feredeului	Iezerul	5346677/1288023	? (1600)	Rock slide	Partial fail	Lesenciuc et al. (2017), Mihu-Pintilie (2018a), Mîndrescu et al. (2013), Stoleriu et al. (2014)
Bolătău L.	Obcina Feredeului	Holohoșca	5327708/1283078	?	Rock slide	Did not fail	Mihu-Pintilie (2018a), Mîndrescu et al. (2013), Stoleriu et al. (2014)
Iezerul Călimani	Călimani Mts.	Puturosu	5266740/1278858	?	Rock slide	Did not fail	Mihu-Pintilie (2018a)
Taul Zânelor	Călimani Mts.	Bistrița	5266840/1257806	?	Rock slide	Did not fail	Decei (1981); Mihu-Pintilie (2018a), Romanescu et al. (2018b)
Izvorul Măgurii	Bârgău Mts.	Leșu	5277968/1243179	?	Rock slide	Did not fail	Decei (1981); Mihu-Pintilie (2018a), Romanescu et al. (2018b)
Dofteana L.	Nemira Mts.	Seaca	5195639/1384520	?	Slide	Failed	Mihu-Pintilie (2018a)
Black L.	Buzău Mts.	Brebu	5115608/1394034	?	Rock slide	Failed	Decei (1981); Mihu-Pintilie (2018a), Romanescu et al. (2018b)
Mocearu L.	Buzău Mts.	Sărățel	5100017/1403183	?	Rock slide	Partial fail	Decei (1981); Mihu-Pintilie (2018a), Romanescu et al. (2018b)
Hânsaru L.	Buzău Mts.	Bâsca	5100313/1394535	?	Rock slide	Partial fail	Decei (1981); Mihu-Pintilie (2018a), Romanescu et al. (2018b)

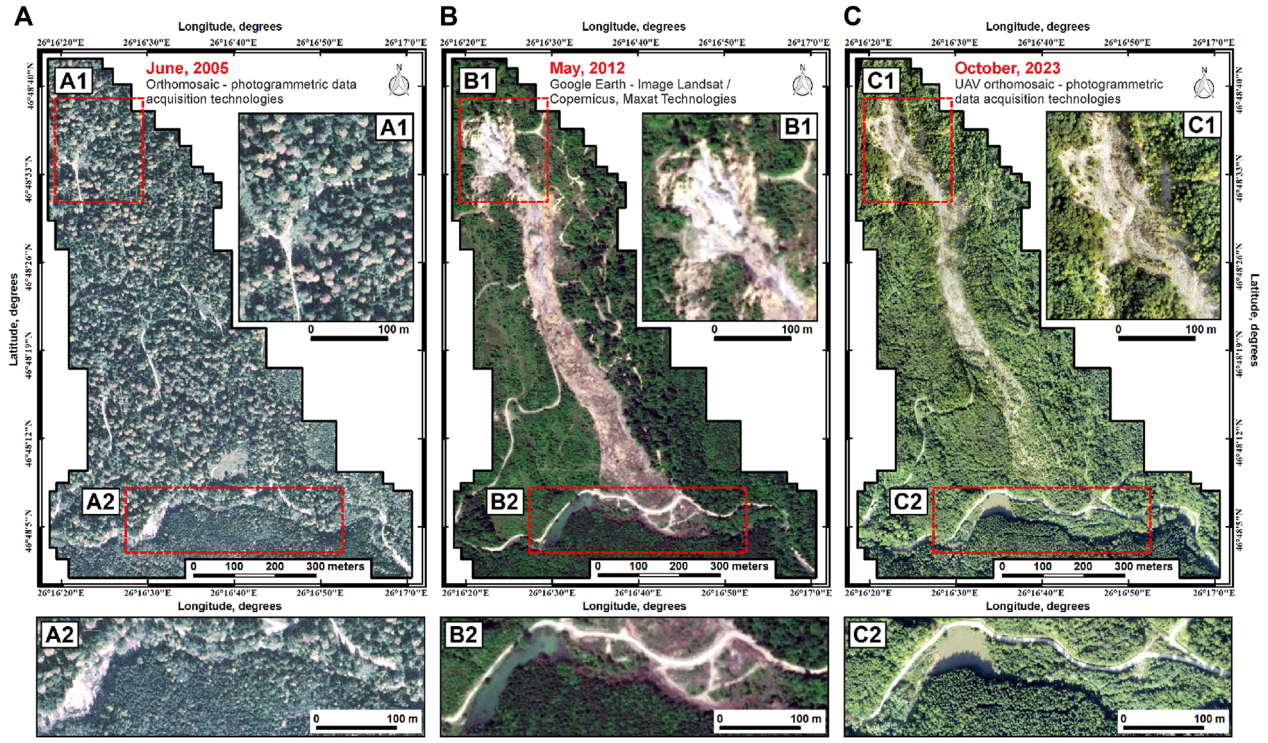

FIGURE 2
Aerial images showing the mountain slope before the landslide-triggered debris flow event **(A)**, the Iapa LDF in 2012 two years after the mass movement occurred **(B)**, and UAV orthomosaic in 2023 **(C)**. The landslide source area **(A1, B1, C1)**, and impoundment/dam area **(A2, B2, C2)** are highlighted in each map.

The Tarcău Nappe, which is of interest for the present study, comprises two main units: the Tarcău Sandstone Digitation, formed by the Lower Tarcău Formation (Paleocene-Lower Eocene); and the Strigoiu Scale, composed of: Putna Formations (Paleocene-Lower Eocene), Straja Formation (Lower Eocene-Middle Eocene), and Ciunget Formation (Lower Eocene-Middle Eocene). The Strigoiu Formation marked the frontal part of the Tarcău Nappe that thrusted towards east the Vrancea Nappe along the Vaduri Digitation (Guerrera et al., 2012). Within this lithological configuration, the landslide that triggered the Iapa LDF in 2010 (Figures 2A, B) occurred in the Ciunget Formation and Straja Formation deposits (Figures 3A, B), very close to the contact with the Putna Formation lithofacies, which consists of dark-greyish clays, calcarenites, and limestone with a thickness of 4-5 m on the left flank of the Iapa LDF (Figure 3C).

The Ciunget Formation (Lower Eocene-Middle Eocene) is represented by a flysch lithofacies with intercalations of microconglomerates and thin layers of red clays. The main predominantly pelitic mass consists of Tarcău sandstones, occurring in beds that reach 10–12 m in thickness. Intermittently, alongside the sandstones, there are also beds of organogenic microconglomerates, with thicknesses ranging from 0.15–0.20 m, containing green schists. Towards the upper part of the lithological succession, there are also beds of friable conglomerates, mainly composed of well-rounded white quartzite fragments, alongside fragments of metamorphic rocks embedded in a silty matrix (Grasu et al., 1988).

The Straja Formation (Lower-Middle Eocene) stands out as a lithological and structural unit marked by a diverse sandstone lithofacies. Therefore, from a petrographic standpoint, the formation exhibits four distinct lithofacies: quartz-arenites, gaizes and spongolites, siltstones, as well as green and dark-red clays (Grasu et al., 1988). The quartz-arenites, which are the main lithological component in the LDF source area, are fine greenish, glassy sandstones with a sharp fracture, form the basal turbidites components. Microscopically, these sandstones predominantly feature quartz grains and cherts, accompanied by lesser amounts of muscovite, feldspars, chloritized biotite, zircon, and pyrite. Gaizes and spongolites make up either the basal layers of specific turbidites or the upper sections in sequences of calcareous microconglomerates and sandstones. Meanwhile, siltstones may manifest as slender interlayers within red and green shale or as more substantial turbidite beds displaying parallel to convolute lamination. In both instances, the matrix is composed of clay-sericite or clay-carbonates. The clays lithofacies encompass a significant proportion, accounting for 62% of the Straja Formation column. In the study area, these clays are observed in distinct layers measuring 5–20 cm, displaying varying shades of red or green (Grasu et al., 1988). However, the stratigraphy of the Tarcău sandstones (Figure 3D) in both the Ciunget Formation and Straja

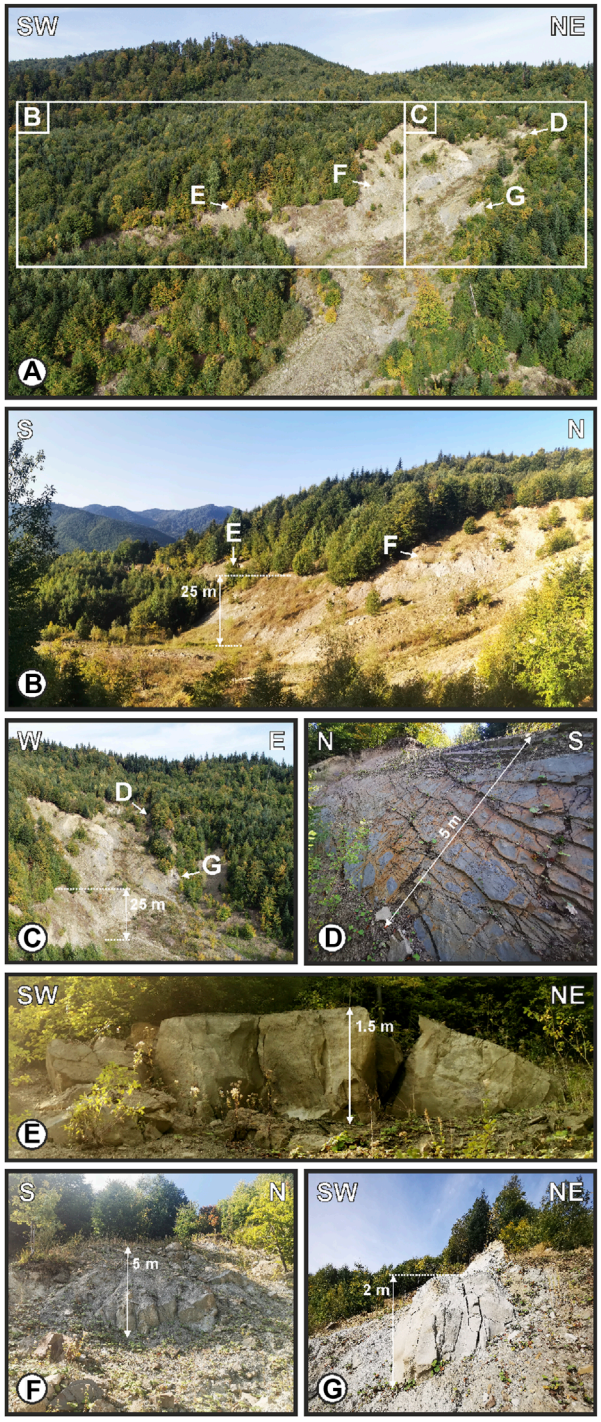

FIGURE 3
Lithology of the Iapa LDF source (see A1, B1 and C1 in Figure 2): **(A)** aerial view of the landslide scarps area near Drumul Chinezilor ridge; **(B)** west; and **(C)** north aerial views of the main scarp area with **(D)** outcrops of Tarcău sandstone of the Straja Formation, and **(E)** medium, **(F)** high, and **(G)** very high desegregated sandstone deposits during the Iapa LDF event.

Formation, with varying thicknesses and hardness (Figures 3E–G), and interspersed with siltstone and clay layers, was the main lithological factor of Iapa LDF event in the synoptic context of the summer of 2010.

2.2 Climate condition

In documenting the direct relationship between climatic conditions and landslide processes that occurred in the upper Iapa watershed, we utilized both general data characterizing the climate on the eastern flank of the Goșmanu Mountains (Apostol, 2004) and local data recorded at the Luminiș pluviometric station (46°48′01″N/26°28′53″E) from the lower Iapa watershed (Cojoc et al., 2015). Therefore, the general climatic characteristics include annual mean temperatures ranging between 5°C (Nechit, 450 m a.s.l.) and 8°C (Săvinești, 280 m a.s.l.) at lower altitudes in the region, and between 2.5°C and 3°C at the meteorological station located above 1,500 m a.s.l. (e.g., Ceahlău Mts.). In both cases, the annual thermal characteristics are associated with a higher value of humidity. The mean precipitation amounts range between 600 mm (Moldavian Subcarpathians) and 900–1,000 mm (upper Iapa watershed). The snow cover duration ranges between 80 and 82 days, but in the case of upper part of the mountains valleys, like the Iapa, Calu and Nechit rivers, the snow cover duration can exceed 90 days due to shelter conditions. Overall, this type of climate is characteristic of mountains with moderate altitudes and corresponds to the mixed forest zone in the Eastern Carpathians (Cheval et al., 2014; Cojoc et al., 2015).

Regarding the precipitation regime in the trigger zone of the Iapa LDF, the data recorded at the Luminiș pluviometric station (300 m a.s.l.) between 1971 and 2021 indicate that the mean precipitation amount is 703.5 mm, with June (108.5 mm) and July (107 mm) being the wettest months of the year (Supplementary Table S1). However, the annual rainfall amount increases with altitude, especially from east to west, where in the study area, these values frequently exceed 1,000 mm. This phenomenon also occurred in 2010, when according to data recorded in Iapa wathershed, 12 km downstream of the Iapa LDF, the annual precipitation amount was 1,007 mm (Cojoc et al., 2015; Romanescu et al., 2018a). Moreover, only during the June-August interval of 2010, when the LDF occurs, the cumulative precipitation amount accounts for 70% of the total precipitation recorded during the entire year. However, this pluviometric regime indicates direct control of climatic conditions on geohazard manifestations (Mihu-Pintilie, 2018a), as well as an indirect causality between the occurrence of landslides and debris flow triggered by extreme rainfall in areas without forest vegetation (Lesenciuc et al., 2017).

2.3 Hydro-morphological characteristics

The Iapa River, along with the Calu River to the north and the Nechit River to the south, are the main tributaries of the Bistrița River from the northeastern flank of the Goșmanu Massif. All three watercourses flow from west to east, perpendicular to the general orientation of geological strata (Brustur et al., 2019). Consequently, the entire hydrographic network is concentrated on the main valley with a few short and low-discharge tributaries. Also, due to the north-south orientation of the geological structures, the main watercourses are segmented by numerous lithological thresholds (e.g., Duraș waterfall on the Iapa River; Brustur et al., 2019).

In this hydro-morphological configuration, the lowest point in the Iapa watershed (76.01 km^2) lies at the confluence of the Bistrița River (264 m a.s.l.), while the highest point is situated in the western part of the basin at Murgoci Peak (1,293 m a.s.l.). The Iapa watershed exhibits a slightly asymmetrical catchment basin, characterized by a parallel hydrographic network type (Jung et al., 2019). The left slope, covering a width of 1–2 km, lacks permanent tributaries. In contrast, the right slope, extending 3–4 km, is drained by several significant streams, including Mânza, Măniș, and Mălina. However, in the area where the LDF occurs, specifically on the southern slope of the Drumul Chinezilor ridge, the hydrographic network consists solely of temporary streams (e.g., Limpedea brook), all of which are collected by the Iapa River. Consequently, the Făgețel Lake, formed by the LDF dam obstructing a 300 m long-section of the Iapa Valley (see A2, B2 and C2 in Figure 2) at 20.5 km upstream of the confluence with the Bistrița River, lacks any other permanent tributary.

Concerning the flow rate data of the Iapa watercourse, groundwater contributes with 40% to the annual discharge (Cojoc et al., 2015). Therefore, from 1950 to 2021, the multi-annual discharge at the Luminiș gauging station averaged 0.63 m^3/s, with a minimum mean discharge rate of 0.2 m^3/s in 2013 and a maximum mean discharge rate of 1.7 m^3/s in 1970 (Supplementary Table S2). However, climatic conditions, which control the rest of 60% of the flow rate and are often influenced by extreme rainfall events, make the maximum discharge data more representative for the present study. In this context, the highest discharge values recorded on the Iapa River at the Luminiș gauge station occurred on 8 June 1969 (75.3 m^3/s), 28 May 1972 (65.8 m^3/s), 12 July 2005 (58.8 m^3/s), and 2 June 2016 (68.6 m^3/s). In 2010, the maximum flow rate was recorded on 26 June, reaching 40 m^3/s. However, a detailed analysis of this flash floods event and its correlation with LDF and Făgețel Lake formation will be detailed in next sections.

2.4 Land use and anthropogenic activity

The vegetation within the upper Iapa watershed consists of 95% mixed forests, and two distinct zones are observed: the spruce zone (*Picea abies*, *Picea excelsa*) and the beech zone (*Fagus sylvatica*), both occasionally associated with herbaceous vegetation. The spruce zone constitutes over 50% of areas situated above 1,000 m a.s.l., particularly in the high and middle sections of the main ridges. Consequently, spruce stands in these zones are either pure or nearly pure, characterized by dense forest masses, with a sparse or underdeveloped herbaceous or shrub layer. At lower elevations (850–900 m a.s.l.), the spruce mixes with fir (*Abies alba*) and beech. Notably, in the area of the landslide source of the Iapa debris flow (875–800 m a.s.l.), pine (*Pinus sylvestris*) also appears. At altitudes ranging from 450 m a.s.l. to 600 m a.s.l., corresponding to the elevation of Făgețel Lake (615 m a.s.l.), the emergence of the beech zone is influenced by continental and foehn-like climatic factors, albeit covering a smaller surface area. In some areas, the beech forests at these elevations also incorporate specimens of elm (*Ulmus montana*) and sycamore (*Acer pseudoplantanus*). Within the shrubbery along the Iapa watercourse, noteworthy species include rowan (*Sorbus aucuparia*), hazel (*Corylus avellana*), spindle (*Euonymus europaea*), red elderberry (*Sambucus racemosa*), and black elderberry (*Sambucus nigra*). However, in the water mass accumulated behind the Iapa LDF dam, of the tree species mentioned earlier, currently, only the trunks of spruce are still visible above the water's surface.

Overall, being an intensively forested area, the main and only industrial activity in the region is the exploitation and valorization of timber. Thus, satellite images reveal numerous areas where the forest has been clear-cut in longitudinal strips towards the valleys of the Iapa, Manzu, and Maniș rivers, extending almost to the alignment of the main ridges. The most heavily exploited area was identified in the upper sector of the Iapa River, specifically on the eastern slope of the Murgoci Peak (1,293 m a.s.l.), the entire left slope of the Mânzu stream (Mânzei ridge), and in the study area, formerly known as the Limpedea logging zone or Drumul Chinezilor ridge. In this context, being an area with limited accessibility and steep slopes, heavy forest tracks was used for timber extraction, forming paths that have turned into deep cutting rigoles, gully and landslide scarps. However, only in the investigated area, the density of the road and paths network used for timber exploitation is 4.5 km/km^2. As we will see in the upcoming subsections, the exploitation paths network and the deforested areas was one of the main factors that triggered the Iapa LDF in the summer of 2010.

3 Data collection and methods

In this study, to generate detailed maps and specific charts, including the geomorphological sketch of the affected area, longitudinal topographic sections and cross-sections, the thickness of erosion and deposition map derived from the difference of two successive DEMs (DOD), and the water surface evolution of the Făgețel Lake from formation to the present, we utilized a variety of data sources such as aerial (Figure 2A) and satellite (Figure 2B) imagery, UAV-derived orthomosaic (Figure 2C) and old cartographic products (topographic maps, scale 1:5,000). Therefore, all data, whether produced during the field survey investigation by direct measurements or acquired from various sources and used as background to highlight the formation and evolution of the Iapa LDF, are detailed in Table 2.

3.1 UAV and field survey investigation

The field survey campaign took place in October 2023 and covered an area of approximately 15 ha on foot and 20 ha through UAV mapping, including the landslide source area, the debris flow paths, the fan area (LDF dam), and the water surface of the impoundment. The primary objective was to investigate the triggering in the crown area, track the flow-slide evolution in terms of both erosion and accumulation, and assess the damage in the flooding area caused by LDF dam formation. All data, including pictures, waypoints, and topographical measurements, were subsequently geolocated using a accurate GPS. Regarding the aerial measurements, the use of UAV techniques was possible in such a forested area due to the fact that the 2010 debris flow-slide event created a scar in the forest vegetation. However, after the rainfall-induced debris flow-slide event in 2010, the broken trees were collected by the forest administrators.

TABLE 2 UAV, satellite imagery and cartographic products used to investigate the Iapa LDF, dam formation and impounded lake evolution.

Data type	Name of cartographic products	Date of acquisition/edition	Source
Aerial imagery	UAV-derived orthomosaic	October, 2023	Field survey, direct acquisition
	Orthophoto (0.5 m resolution)	June, 2005	
Satellite imagery	Orthophoto (2 m resolution)	May, 2012	Google Earth satellite view
		April, 2014	
		May, 2017	
		September, 2019	
	Landsat 7 ETM+ normalized difference moisture index (50 m resolution)	03 July, 2010	Copernicus Open Access Hub
		20 August, 2010	
Topographic map, scale 1:5,000	L-35-041-D-a-1-III	1975	National Agency for Cadastre and Land Registration of the Borrower, Neanț County, Romania
	L-35-041-D-a-1-IV		
Topographic map, scale 1:25,000	L-35-041-D-a	1984	National Agency for Cadastre and Land Registration of the Borrower, Neanț County, Romania
Geological map, scale 1:50,000	Sheet 48 days Tazlău (L-35-41-D)	1983	Geological Institute of Romania

Currently, the forest growing on the surface of the LDF is young and dispersed.

The photogrammetric data acquisition stage consisted of using a high-performance DJI Phantom 4 Pro drone with a full-frame digital camera with a 20-megapixel CMOS sensor. The flight plan was designed to perform successive flights with 70% overlap between photos. Flights were conducted at a relative altitude of 110 m above the slope where the Iapa LDF occurred, correlated with mountain topographic variation, in order to obtain a ground sampling distance (GDS) of 2 cm. The photogrammetric area surveyed is 20 ha, of which the affected area by debris flow-slide is 13.5 ha and by flood approximately 2.5 ha. The photos obtained are automatically georeferenced by the drone using the on-board RTK system to record precise geographic coordinates for each photo. A total of 571 photos were obtained, which were processed using automated procedures with appropriate spatial alignment algorithms. In Figure 4A the Projection Center Point (PCPs) coordinates of each UAV photo are indicated.

The dense point cloud, mesh, texture, tiled model and digital surface model (DSM) algorithms implemented in Agisoft Metashape Pro v.1.6.5 software were used to produce the orthomosaic (2 cm spatial resolution) (Figure 2C) and UAV-derived DSM (10 cm spatial resolution) of the Iapa LDF area. Spatial analyses were performed using Esri ArcGIS v.10.2. The DSM was resampled to a spatial cell size of 1 m^2. In the final stage of data processing, to capture all topographic details within and in the vicinity of the LDF body, the final DEM was filtered to exclude vegetation (e.g., trees, shrubs) or any other point elevation that does not relate to the land surface (Figure 4A).

3.2 DEM-derived from old maps and DOD

In order to obtain the thickness of erosion and deposition map derived from the difference of two consecutive DEMs (DOD) (De Falco et al., 2023), an elevation model before the Iapa LDF event was needed for comparison with the UAV-derived DEM obtained for 2023. Therefore, the best option for extracting altitudinal information was the topographic maps at a 1:5,000 scale, considering the low resolution of other available elevation models like SRTM or ASTER (Khasanov, 2020) in the investigated region. In this context, two topographic maps corresponding to the study area were acquired from the National Agency for Cadastre and Land Registration of Neamț County, Romania (Table 2). The contours with 2.5 m equidistance were manually digitized, along with other point elevation information (e.g., mountain peks, elevation of hydrographic network), using the old maps as a background. Based on this shapefile elevation data, a DEM with a 1 m cell size, similar to the resolution of the UAV-derived DEM, was generated using the Topo to Raster interpolation tool in ArcGIS 10.2 (Figures 4B, C).

Regarding the DOD methodology, which is a widely adopted tool for volumetric data in geomorphic change detection (GCD) (De Falco et al., 2023), especially in areas affected by landslides (Jaboyedoff et al., 2012) and debris flows (Bull et al., 2010; De Long et al., 2012), it was employed to identify the primary areas of erosion and accumulation in the case of the Iapa LDF. The difference between the 2023 UAV-derived DEM and the 1975 old maps-derived DEM was computed using the Raster Calculator tool in ArcGIS 10.2 (Figure 4D). The resulting raster was used to obtain morphometric values for the detached, transported,

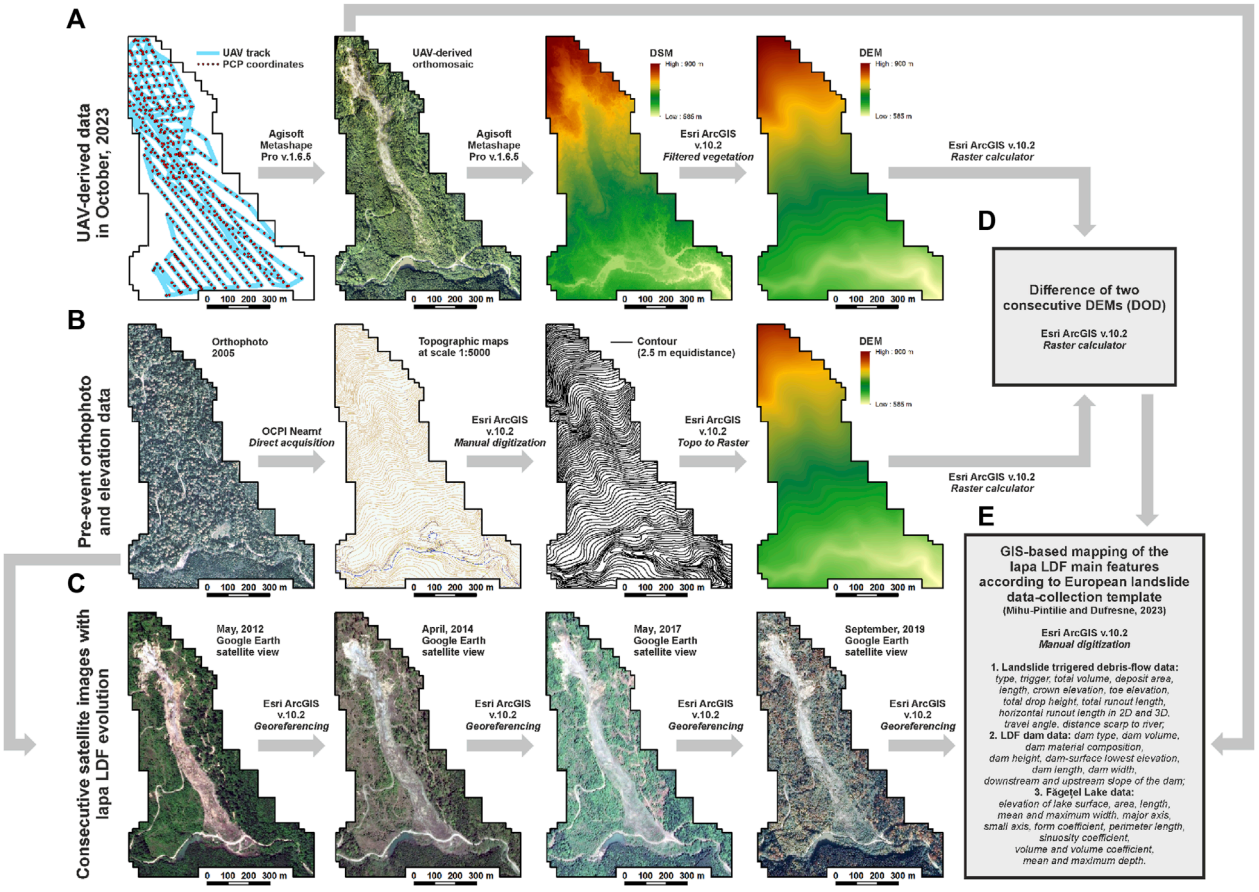

FIGURE 4
Workflow chart followed in this study to obtain the Iapa LDF geodetic data: **(A)** The area covered by 2023 UAV measurements, including PCP coordinates of each vertical photo, the UAV-derived orthomosaic, DSM derived from UAV survey, and the resulting DEM obtained after filtering the DSM to exclude vegetation and other non-elevation surfaces; **(B)** Pre-event orthophoto, the 2.5 m equidistance contours manually digitized using old topographic maps as background, and the resulting DEM with pre-event slope characteristics; **(C)** Consecutive satellite images (Google Earth georeferenced screenshots) used for the evolution characterization of the Iapa LDF; **(D)** Difference (DOD) between the 2023 UAV-derived DEM and the old maps-derived DEM used to delineate erosion and deposition areas; **(E)** GIS-based mapping of the Iapa LDF according to the European landslide data-collection template (Mihu-Pintilie and Dufresne, 2023).

and deposited terrigenous material. Additionally, it facilitated the accurate delineation of the morphological features of the Iapa LDF. Furthermore, by utilizing successive Google Earth satellite views from 2010 to the present (Figure 4C), along with DOD data, we managed to identify other episodes of debris flow-slide that occurred in the crown area of the Iapa LDF after the 2010 event.

3.3 Hydro-morphological data collection

The delineation of the Iapa LDF features for hydrological and geomorphological mapping was conducted through field descriptions correlated with the geodetic data (e.g., UAV-derived orthomosaic and DEM). The measurements improve the estimate of the shape, surface area, and volume of both the initial and recently reactivated debris flow-slide in the study area. Moreover, since the present case study will be included together with other examples in an upcoming European landslide dams database, the delineation of geomorphological features to obtain accurate morphometrical values was achieved according to a specific data-collection template (Mihu-Pintilie and Dufresne, 2023) (Figure 4E). The summary of this data-collection includes informations related with: 1) Landslide triggered debris-flow data: type, trigger, total volume, deposit area, length, crown elevation, toe elevation, total drop height, total runout length, horizontal runout length in 2D and 3D, travel angle, distance scarp to river (Cruden and Varnes, 1996; Hungr et al., 2014); 2) LDF dam data: dam type (Costa and Schuster, 1988), dam volume, dam material composition, dam height, dam-surface lowest elevation, dam length, dam width, downstream and upstream slope of the dam (Fan et al., 2020); 3) Făgețel Lake data: elevation of lake surface, area, length, mean and maximum width, major axis, small axis, form coefficient, perimeter length, sinuosity coefficient, volume and volume coefficient, mean and maximum depth (Mihu-Pintilie, 2018b; Romanescu et al., 2018b).

4 Results and discussions

4.1 The rainfall-triggered Iapa LDF event

As presented in the introduction section, during the summer of 2010, significant heavy rainfall impacted the northeastern part of the Goșmanu Massif, leading to several flash floods along the Iapa Valley. The highest precipitation amounts were recorded in three intervals: 16–22 May (115.8 mm), 22–27 June (195.8 mm), and 25–27 July (70.4 mm). Overall, from May to August 2010, the cumulative precipitation amounted to 599.1 mm, which represents 70% of the total precipitation recorded throughout the entire year (Figure 5A). These weather conditions also induced historically high discharge rates on the Iapa River as a response to rainfall events: 16.4 m^3/s on 22 May, 40 m^3/s on 26 June, and 12.6 m^3/s on 27 July (Figure 5B). According to locals, during these periods, the Iapa River flooded several courtyards and damaged several bridges and roads in settlements downstream of the Iapa LDF location, especially in Neguleşti and Luminiș.

However, based on discussions with stakeholders, including the foresters whose ranger office house is located 8 km downstream from the LDF dam, it could not be precisely determined which of the three rainfall events triggered the debris flow-slide event. Under these circumstances, we attempted to correlate satellite imagery with the possible weather interval when the mass-movement occurred. Therefore, due to the fact that the Iapa LDF event left a scar in the forest vegetation, the best option was to investigate successive Landsat 7 ETM+ Normalized Difference Moisture Index (NDMI) images with a resolution of 50 m per pixel (Figure 5C). In practice, NDMI is generally used to determine vegetation water content (Ochtyra et al., 2020), which, in the case of the present study, can indicate when forest vegetation was removed from the area affected by the debris flow-slide. In this framework, the analysis of NDMI rasters indicates that the Iapa LDF occurred between 03 July and 20 August, and most probably the rainfall event from 27 July was the one that triggered the LDF. Furthermore, even though the most severe meteorological conditions of 2010 were not recorded at that time, the initiation of landslide processes can be attributed to the 27 July event, although the decisive factor was the large quantities of precipitation that saturated and weighed down the southern slope of Drumul Chinezilor ridge throughout the entire summer season.

Interestingly, it should be noted that during the period of 25–27 July 2010, when it is also considered that Făgețel Lake was formed, the discharge data on the Iapa Valley did not show a proportional increase directly corresponding to the amount of precipitation that fell, as was the case with previous rainfall events. In this context, we consider that the blocking of the Iapa Valley by the LDF fan caused the accumulation of water behind the dam, creating a delay of several hours between the high quantities of precipitation and the discharge response. This delay most likely corresponds to the filling duration of the newly formed lacustrine depression, estimated to be between 2 and 4 h. After the watercourse resumed its flow over the dam surface, the discharge data recorded at the Luminiș gauge station showed a progressive increase, reaching a maximum of 12.6 m^3/s.

4.2 DOD-base LDF characteristics

The difference of DEMs (DOD) methodology used for GCD across the Iapa LDF area was primarily applied to obtain volumetric data and secondarily to confirm the field survey observations and measurements. In this regard, the difference between the two rasters of 2023 UAV-derived DEM and the 1975 old maps-derived DEM indicates a total volume of 782,500 m^3 of displaced materials, of which more than 450,000 m^3 represents the volume of the Făgețel Lake dam. The erosion and deposition thickness values range between −28 m in the source area and +30 m in the deposition area (Făgețel Lake dam). The mean thickness value is approximately ±3.4 m, suggesting that, apart from the crown area and the obstructed river sector where the erosion and accumulation amplitudes are high, the rest of the Iapa LDF exhibits a relatively shallow depth configuration (Figure 6A).

The cross section locations of the field observations and UAV-derived GPS measurements used to validate the DOD outcomes are also indicated in Figure 6B. They show values ranging between 15 m and 25 m of erosion in the landslide-triggering area and on the debris flow-slide flanks, while erosion values ranging between 2 m and 4 m are observed in the main channel of the flow-sliding area. Regarding the deposition values, they are more representative in the LDF dam area, where the flow-slide accumulation reported thickness exceeding 25 m between the valley floor and the top of the obstructed dam. However, when comparing the field measurement results with the DOD values, the errors do not exceed 1 m, especially in the deposition area, and this is a consequence of the fact that direct measurements could not capture the entire flow-sliding plane at all analyzed points. In the erosional area, the errors were minimal (less than 0.5 m), including here also the debris flow events post-2010, which are quite visible in the LDF source area.

Overall, the DOD map accurately indicates all details related to the thickness of the mass movement in terms of erosion and accumulation areas. This analysis permitted the identification of important geomorphological aspects, such as the presence of channels where major erosion occurred (C1–C7), the first slope change at the foothill (C8), the upper part of the debris flow-slide area (C9–C12), or the precise limit of the obstructive dam (C13–C15) (Figure 6B).

4.3 Hydrological and geomorphological characterization of Iapa LDF

For a more comprehensive hydrological and geomorphological characterization of the Iapa LDF, we divide the investigated area into three landform parts: 1) Landslide triggered debris-flow area; 2) Iapa LDF dam area; 3) Lake area. All morphometric values will be recorded in an upcoming landslide dams database, alongside other representative landslide.

4.3.1 Landslide source and debris-flow area

The topography of the south-facing slope of the Drumul Chinezilor ridge, loose material on its surface and anthropogenic impact as a consequence of intensive deforestation provide very

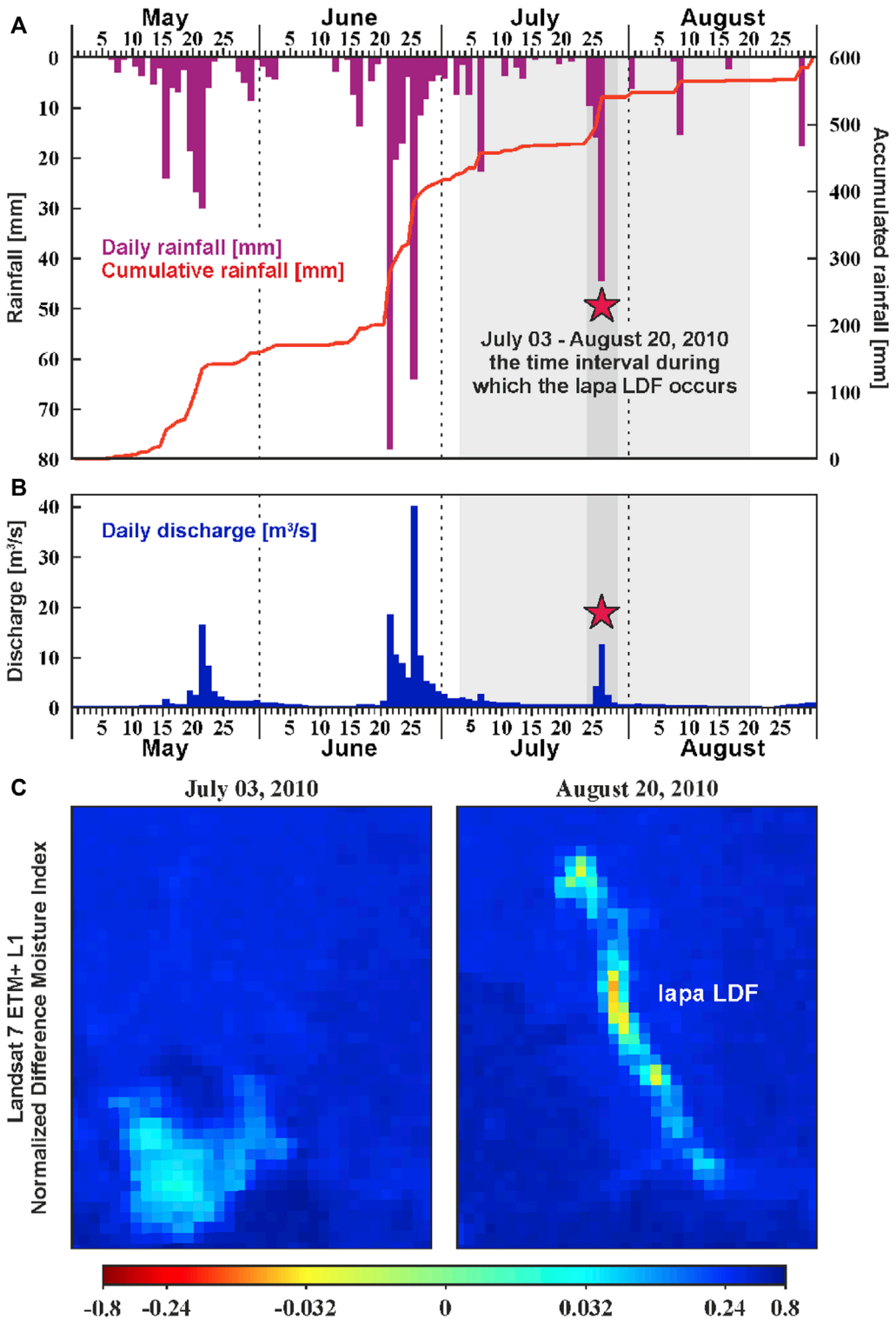

FIGURE 5
The rainfall event that triggered the Iapa LDF: daily and cumulative precipitation (mm) in the May–August interval of 2010 **(A)**, and correlation with daily maximum discharge (m^3/s) at the Luminiș gauging station (see Figue 1C) **(B)**. In **(C)** Landsat 7 ETM+ L1 NDMI imagery indicating that the Iapa LDF occurred between July 3 and August 20 interval of 2010. The red star indicates July 27 as the most probable date.

favorable conditions for a wide range of geomorphological processes such as landslides and debris flows (Figure 7A; Table 3). Therefore, the landslide process that triggered the debris flow-slide in 2010 started at an altitude of 875 m a.s.l. and affected an area of 13.5 ha. The height of the main scarps ranges from 25 m in the central part of the crown area to 10 m on the secondary scarps located on both

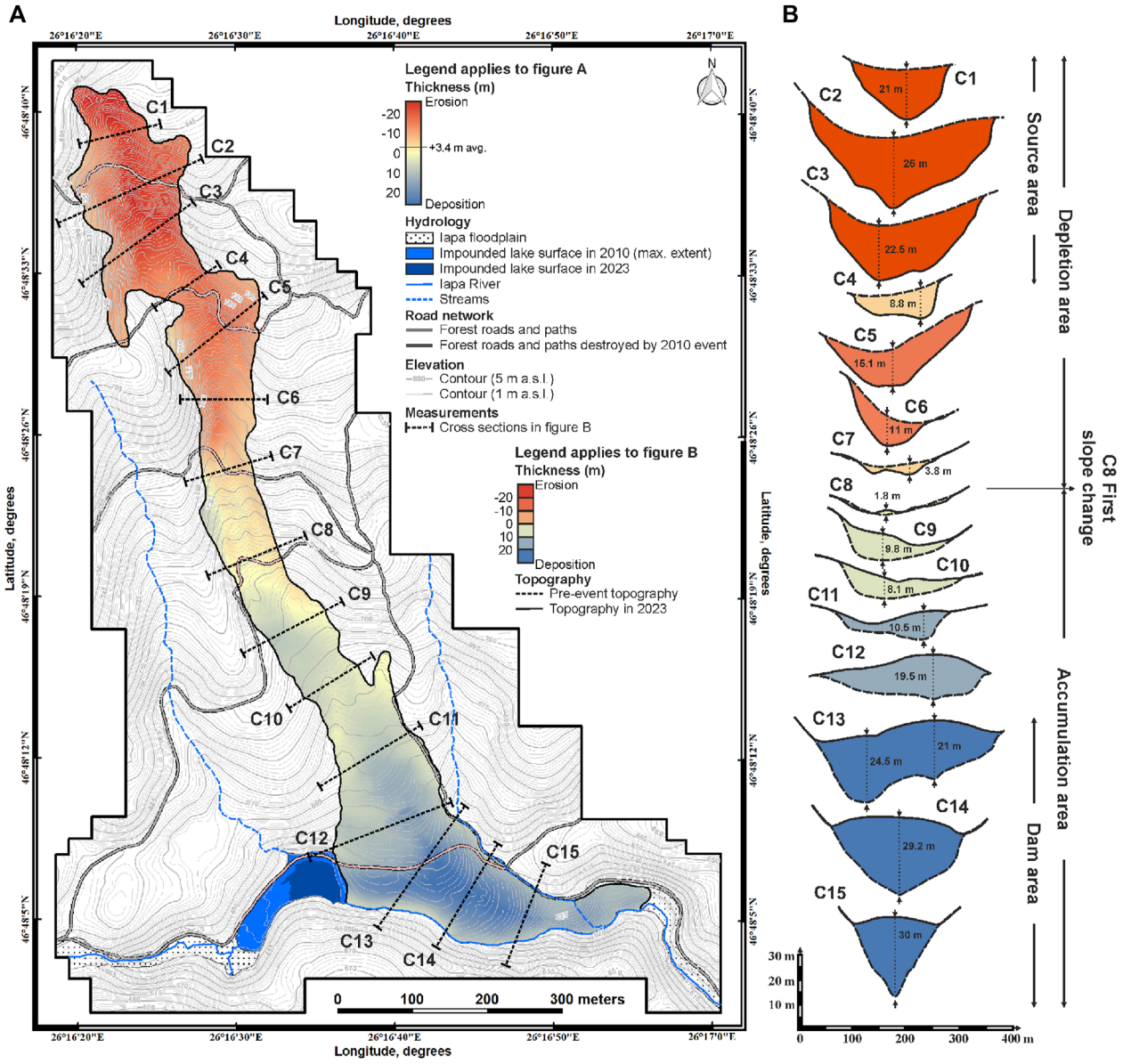

FIGURE 6
The difference of DEMs (DOD) map of the Iapa LDF **(A)**. In **(B)**, 15 transversal cross sections highlight the main erosion and deposition areas along the affected slope.

flanks of the landslide depression. The slope of the main scarps ranges between 60° and 90° and are still very active (Figure 7B).

The debris flow-slide area started in two confined channels and joined in the middle of the landslide depression at 780 m a.s.l., approximately 300 m below the upper limit of the crown area. The slope consists of very poorly sorted sediments with a predominance of sand and sandstone clasts, making it particularly susceptible to flow-sliding processes. For this reason, the investigated mass-movement was classified as a debris flow-slide based on sediment texture, geomorphological characteristics of both depletion and accumulation zones, and especially due to the rapid course of the flow-slide event. Furthermore, the presence of erosional channels and small debris fans formed post-2010 in the initial landslide area indicates that the current processes belong only to the channelized form of debris flow.

The depletion zone comprises a steep scarp and multiple old-to-new channel-like transport areas, deeply incised into the valley slope. The slope gradient is highest in the upper part and gradually diminishes further down the slope. The rugged relief of the depletion area is accentuated by the presence of structural steps, leading to significant changes in slope gradient. For instance, the floor of the middle channel incision descends by 5 m as it traverses the bedrock outcrop in the central part of the depletion zone. The depth varies along the central line in the upper part of the depletion zone and along the two lateral channels after the main channels split 180 m before the onset of the debris flow

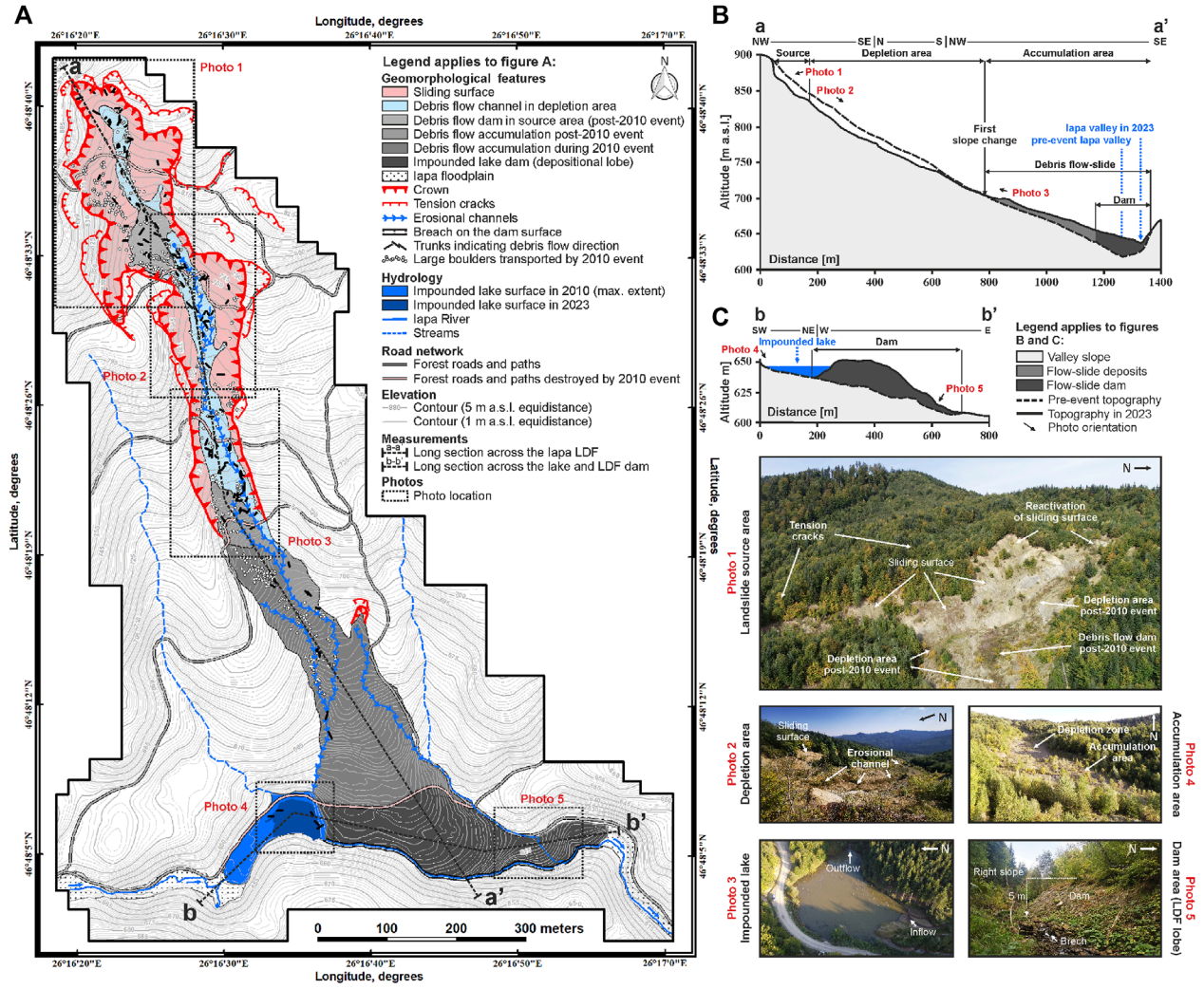

FIGURE 7
The simplified geomorphological sketch of the Iapa LDF **(A)**. Long section (a-a') across the landslide source area, depletion zone, and accumulation area (vertical exaggeration 1:2.5) **(B)**. Long section (b-b') across Făgețel Lake and debris flow-slide dam (vertical exaggeration 1:3) **(C)**. The main morphological features indicating the slope failure processes and the main debris flow characteristics are highlighted in photos.

accumulation. The maximum width of the depletion zone measures 90 m, while its length along the central line extends to 490 m. The elevation difference between the upper and lower parts is approximately 85 m a.s.l.

The debris flow-slide accumulation area begins in the lower part of the depletion zone. The upper part of the accumulation has an elongated fan shape that transforms into a lobe-like accumulation confined within the Iapa Valley. In the longitudinal section a–a' measured across the entire Iapa LDF area, the current topography of the fan surface indicates a relatively 15° gradient, characteristic of fans resulting from flow-sliding processes (Figure 7B). The lower part of the accumulation area indicates that deposits impacted the right slope of the Iapa Valley during the 2010 event. However, in October 2023 when field measurements were conducted, the materials impinged on the opposite slope had mostly eroded due to changes in Iapa watercourses on the dam surface. Additionally, the lateral development of the accumulation front, measured from the apex, is considerably larger on the right side, in the direction of the Iapa River flow. This asymmetry indicates both the transport capacity during flood events and the dynamic processes of debris flow, which continued for approximately 100 m along the valley. Overall, the Iapa LDF transported a large amount of material for over 750 m, with the total length of the accumulation from the upper part to the obstructed river bed being 550 m, and 200 m along the Iapa Valley. The maximum width reaches 330 m, with a thickness of about 30 m in the dam area. The matrix-rich debris flow contains large floating sandstone boulders, most of them concentrated at the toe of the debris flow. However, a significant area of large boulders is also located in the upper part of the accumulation area, indicating other post-2023 mass movements of lesser intensity. Along the long section of the lobe, the variety of clasts indicates a cohesive type of debris flow. Overall, the total volume of the accumulation area is 782,500 m^3 (Figure 7A; Table 3).

TABLE 3 Morphometric characteristics of the Iapa LDF area.

Parameter of Iapa LDF	Value
Affected area (A_{LDF})	13.5 ha
Deposit area (A_D)	8.1 ha
Deposit length (L_D)	750 m
Landslide crown elevation (LC)	875 m a.s.l.
Landslide toe elevation (LT)	615 m a.s.l.
Drop height (H or LC/LT)	260 m a.s.l.
Total runout length (L)	1,250 m
Horizontal runout length in 2D (L_{2D})	1,320 m
Horizontal runout length in 3D (L_{3D})	1,400 m
Travel angle (H/L)	0.26
Distance scarp to river (L_{sr})	1,160 m
Volume of displaced materials (V_D)	782,500 m^3

TABLE 4 Morphometric characteristics of the dam area.

Parameter of the dam	Value
Dam area (A_{dam})	2.5 ha
Percentage of LDF deposit area	30%
Dam height (H_{dam})	30 m
Dam-surface lowest elevation (D_{low})	615 m a.s.l.
Dam-surface height elevation (D_{high})	654 m a.s.l.
Dam length (L_{dam})	50 m
Dam width (W_{dam})	330 m
Downstream slope	35°
Downstream slope length	270 m
Upstream slope	65°
Upstream slope length	60 m
Dam volume (V_{dam})	450,000 m^3

4.3.2 Iapa LDF dam area

Generally, a landslide dam is the lower part of the accumulation area, which forms a barrier that can hold back water above the obstructed river level (Fan et al., 2020). In this context, the most widely accepted morphological characterization involves the shape, size, and composition of landslide dams in relation to the size of the blocked valley (Costa and Schuster, 1988). In the case of the Iapa LDF, the obstructed dam is represented by the lower part of the debris lobe, which fills the Iapa Valley. The accurate delineation of the initial shape of the obstructed valley sector was performed in ArcGIS based on the 1975 old maps, also used for DOD. Therefore, according to Costa and Schuster (1988) landslide dam classification, the Iapa LDF dam falls into the second category of dams, occupying the entire section of the obstructed valley. The matrix composition of the dam is mixed, ranging from 1 m floating sandstone boulders to fine debris deposits resulting from disaggregated sandstone, siltstone and clay rocks and topsoils transported during the LDF event. However, due to the mass movement type, together with the dam's lithological characteristics and the fact that it formed a long-term lake, the Iapa LDF is quite unique in the landscape of the Eastern Carpathians. Usually, the other examples of landslide dams that did not fail after a few days have been formed by rock slides, which confer high stability due to the lithological composition and morphological characteristics (Mihu-Pintilie, 2018a; Romanescu et al., 2018b).

Regarding the morphometric parameters of the Iapa LDF dam, the surface is 2.5 ha (30% of the accumulation area), and the volume was estimated to 450,000 m^3. The maximum dam height is 30 m, measured from the initial dam apex (654 m a.s.l.), now 4 m flattened by the reconstruction of the road destroyed during the 2010 event, down to the corresponding lower elevation of the Iapa riverbed. At present, the dam surface elevation ranges from 650 m a.s.l. to 610 m a.s.l. The maximum length of the dam, which corresponds to the maximum width of the filled river sector, is around 50 m. The dam width measured from the impounded lake outflow location up to the downstream limit of the dam is 330 m, of which the upstream slope is short (60 m) and steep (65°), and the downstream slope is much longer (270 m) and less steep (35°) (Figure 7C; Table 4).

Regarding dam stability, the main erosional process is the overtopping, represented by the Iapa watercourse, which creates a channel 1.5 m deep and 5 m wide on the dam surface. However, despite the erosive down-cutting, this breach ensures the drainage of water from Făgețel Lake, particularly during periods of rainfall, thereby mitigating flash floods. Additionally, the entire surface of the dam has been replanted with trees, which currently provide additional stability to the dam due to the root network that anchors the upper part of the dam, and by attenuating the direct impact of precipitation.

4.3.3 Iapa LDF lake area

In the case of the lakes formed behind the landslide dams, various terms have been adopted in the scientific literature (e.g., landslide lake, impoundment lake, landslide-dammed lakes) (Fan et al., 2020). In this approach, we consider the most appropriate term to describe the uniqueness of Făgețel Lake as the landslide-triggered debris flow-slide lake, or abbreviated LDF lake. Related to the hydronym Făgețel Lake, this name was given by the locals because the place where the lake formed was previously known as a young beech forest area ("fag" means "beech" in Romanian).

Related to the morphometrical parameters of the LDF lake, in 2023, when the UAV and field survey were carried out, the surface area of the lake was much smaller than its initial size. Therefore, in the following, we will present the morphometric parameters of the lake 2 years after its formation using satellite images available on

TABLE 5 Evolution of morphometric and morpho-bathymetric parameters of the Făgețel Lake.

Parameter of the lake	Year 2010	Year 2023
Elevation of lake mirror	651 m a.s.l	645 m a.s.l.
Water surface (A_{lake})	9,500 m^2	3,100 m^2
Length (L_{lake} or A/W_{avg})	250 m	90 m
Maximum width (W_{max})	60 m	55 m
Average width (W_{avg} or A/L)	38 m	34.4 m
Major axis (AX_{max})	210 m	68 m
Small axis (AX_{small})	78 m	44 m
Form coefficient (AX_{small}/AX_{max})	0.32	0.61
Perimeter length (P)	600 m	260 m
Sinuosity coefficient ($P/\sqrt{3.14A}$)	3.47	2.63
Volume (V)	50,000 m^3	10,000 m^3
Maximum depth (H_{max})	10 m	6 m
Average depth (H_{avg} or V/A)	5.3 m	3.2 m
Volume coefficient ($3H_{avg}/H_{max}$)	1.59	1.6

the Google Earth platform, as well as the morphological parameters measured in 2023 (Figure 4C; Table 2). In this context, the initial surface area of the lake mirror was estimated at 9,500 m^2, with a length of 250 m and a maximum width of 60 m. In October 2023, these parameters had drastically decreased (surface area 3,100 m^2, length 90 m), except for the width, which remained the same. The perimeter of the lake also experienced the same decreasing trend, respectively from 600 m to just 260 m. The considerable reduction in the water surface area is a consequence of the breach on the surface of the dam, leading to a decrease in the maximum depth from 10 m (651 m a.s.l. of the water surface) to only 6 m in 2023 (645 m a.s.l. of the water surface). As for the volume of water at the time of dam formation, it was estimated around 50,000 m^3, but in 2023, it had reduced to only 10,000 m^3. Additionally, the shape of the lake has changed considerably, transitioning from an elongated shape along the flooded valley (sinuosity coefficient of 3.47) to an almost circular shape in 2023 (sinuosity coefficient of 2.63). This trend is also indicated by the ratio of the major and minor axes of the lake, which reveals an evolution of the form coefficient from 0.32 in 2012 to 0.61 in 2023, but not by the volume coefficient, which remains constant around 1.6 values. The volume coefficient indicates that the Făgețel lacustrine basin evolution is very similar to other landslide lakes in the Eastern Carpathians, which maintain the maximum depth at the bases of submerged dam slopes and a constant ratio between the volume and area of the lake. However, the comprehensive evolution of all morphometric and morpho-bathymetric parameters of Făgețel Lake is presented in Table 5.

According to the evolution of morphometric and morpho-bathymetric parameters of Făgețel Lake, our estimation of the lake's lifespan is approximately 20 years (another 6 or 7 years from now) (Figure 8). However, this theoretical estimate does not account for the reactivation of landslide processes, dam destruction due to a major flash flood event, or anthropogenic intervention. All of these factors could lead to the evacuation of water within a few hours or maintain water retention at current levels for an extended period. In either scenario, the hydrological hazard posed by dam destruction no longer represents a threat to population located downstream of the lake due to the considerable reduction of the stored water volume. In any case, it appears that local authorities are making efforts to maintain the lake at its current parameters by clearing trees from the water body, landscaping the shores and access routes to the lake, as well as managing forestry waste.

4.4 Lessons learned

The location of the Iapa LDF in the flysch zone of the Eastern Carpathians, a mountainous area frequently affected by extreme rainfall events with high erosional impact in deforested locations, constitutes the main premise for triggering the recent mass-movement processes that have occurred in the upper Iapa Valley. Even though the debris flow-slide event that occurred in the summer of 2010 was extremely dynamic, a stabilized appearance of vegetated landforms in the LDF accumulation area indicates that shallow landslides and debris flows are currently active only in the source and depletion area. However, a new episode of heavy rainfall that affected the southern slope of the Drumul Chinezilor ridge can occur at any time. This hazard threat arises from the analysis of climatic conditions during the May-August period of 2010 when the time lag between the long-lasting rain culmination and the landslide triggering suggests that the debris flow-slide initiation was connected with cumulative precipitation over the 3 months in the study area. Therefore, lessons learned and future actions needed to prevent the further reactivation of the Iapa LDF suggest that local authorities should avoid clear-cutting forests on exposed slopes prone to landslide processes. Additionally, the network of forest exploitation paths should be minimized on steep slopes, as the density of these timber transportation routes has been the primary anthropogenic trigger leading to the occurrence of the Iapa LDF.

Regarding the Iapa River sector obstructed by 2010 LDF event and the formation of Făgețel Lake, although this type of landslide lakes are not unique in the landscape of the Eastern Carpathians, the uniqueness and hazardous threat arise from the dam composition and stability characteristics. Usually, the lifespan of dams formed by debris flow-slide processes is short (a few hours) due to the low cohesion of the debris matrix. Therefore, the long-term presence of Făgețel Lake and the relatively stability of the dam indicate, but only in this case, that the potential flood hazard threat was partially diminished. However, this does not guarantee that in the event of other similar occurrences, the formed dams will not fail, affecting the population located downstream. For this reason, in the watershed of the Iapa river, in addition to the area affected by debris flow-slide in 2010, other areas susceptible to landslides should also be monitored in the future. In this study, we identified three possible other areas where mass movement processes could occur on a similar or even

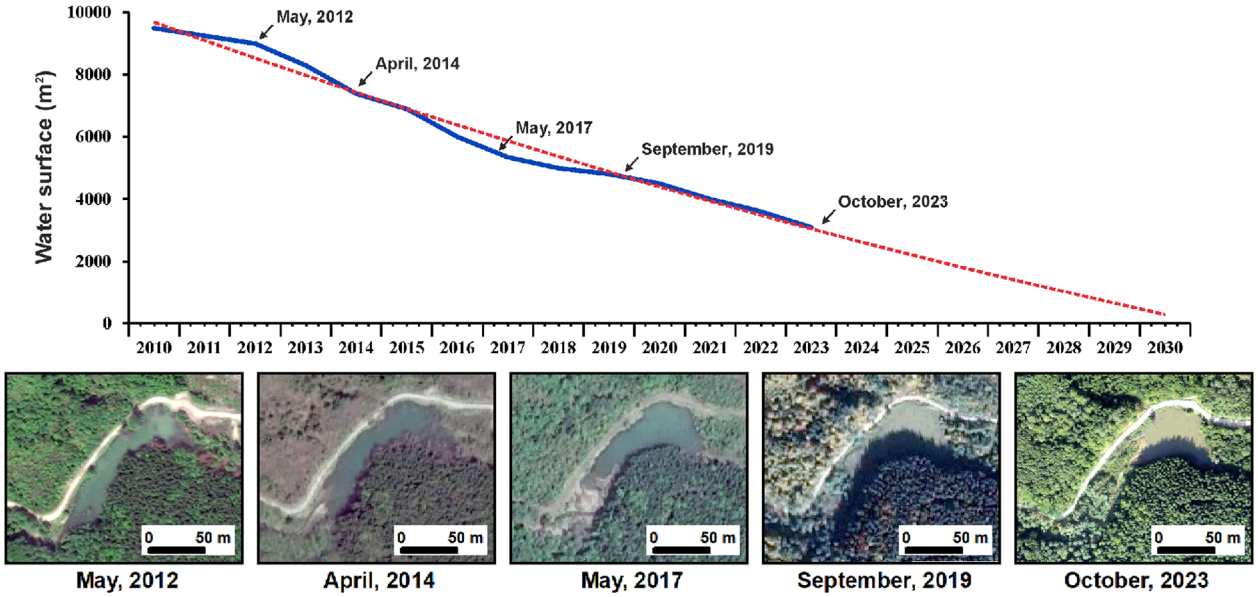

FIGURE 8
Water surface evolution of the Făgețel Lake between 2010 and 2023 (blue line) and the lifespan estimation (dotted red line) using water surface extent delineated based on five consecutive aerial images.

larger scale than Iapa LDF. However, we anticipate that the outcomes of this approach will aid in enhancing the emergency response plan in the event of any other potential destructive hydro-morphological events linked to heavy rainfall in the surveyed region.

4.5 Limitation of UAV survey methodology

From the perspective of UAV survey methodology used in this study, both for extracting the main morphological and morphometric parameters of the Iapa LDF and for understanding the mechanism of the impoundment and formation of Lake Făgețel, there were several limitations that need to be addressed. The UAV survey conducted to obtain a DEM as accurate as possible with the topographic reality in 2023 was hindered by the forest vegetation that had spread over the area. This aspect made the generation of the DEM using DTM-derived from successive orthomosaic aerial images a time-consuming process, involving the identification and filtering of non-elevation data (e.g., tree canopy). However, in the future, we intend to use LiDAR technology to reconstruct the terrain elevation model in the area affected by the Iapa LDF, a technology that will streamline both the processing and filtering stages of geospatial data, significantly improving the accuracy of the resulting DEM. Despite these drawbacks, the use of DEM-derived from UAV survey and corrected on the ground with GPS measurements has yielded satisfactory results.

5 Conclusion

The mass movement that occurred on July 27, 2010, in the upper Iapa Valley (Goșmanu Massif, Eastern Carpathians) can be classified as a landslide triggered debris flow (Iapa LDF). The landslide that triggered the debris flow processes began at an altitude of 875 m a.s.l., affecting an area of 13.5 ha and transporting a large amount of material for over 1.4 km up to 615 m a.s.l. The total volume of transported material was approximately 782,500 m^3. The lower part of the accumulation area, namely, the dam area (450,000 m^3), filled a 330 m narrow sector of the Iapa watercourse and formed an impoundment. The water storage above the debris flow-slide dam caused the formation of a elongated lake (250 m length, 9,500 m^2 water surface), currently known as Făgețel Lake. Measurements conducted in 2023 using UAV survey indicate that the lake size has drastically reduced, with the current water surface area being only 3,100 m^2. This considerable reduction is a consequence of the breach on the dam surface, leading to a decrease in maximum depth from 10 m to only 6 m in 2023. Under these morphological and hydrological conditions, the lake is projected to be completely drained in 6 or 7 years.

Overall, being a consequence of extreme rainfall events with high erosional impact in deforested locations where Iapa LDF occurred, the entire area affected by mass-movement remains vulnerable to reactivation under similar rainfall-induced landslide conditions, as observed in 2010 (599.1 mm cumulative precipitation recorded in the May to August interval). Therefore, future actions necessary to prevent further reactivation of the Iapa LDF suggest that local authorities should stop the clear-cutting forests on exposed slopes prone to landslide processes. Additionally, the network of forest exploitation paths should be minimized on steep slopes, as the density of these timber transportation routes has been the primary anthropogenic trigger leading to the occurrence of the Iapa LDF. Furthermore, while the long-term presence of Făgețel Lake and the relative stability of the dam indicate, but only in this case, a partial diminishment of the potential flood hazard

threat, it does not guarantee that formed dams will not fail in other similar occurrences, potentially affecting downstream populations. Therefore, in the Iapa watershed, areas susceptible to landslides should be continuously monitored in addition to the area affected by the 2010 debris flow-slide for future risk mitigation efforts.

Data availability statement

The original contributions presented in the study are included in the article/Supplementary Material, further inquiries can be directed to the corresponding author.

Author contributions

AM-P: Conceptualization, Data curation, Formal Analysis, Funding acquisition, Investigation, Methodology, Project administration, Resources, Software, Supervision, Validation, Visualization, Writing–original draft, Writing–review and editing. CS: Conceptualization, Data curation, Formal Analysis, Funding acquisition, Investigation, Methodology, Project administration, Resources, Software, Supervision, Validation, Visualization, Writing–original draft, Writing–review and editing. AU: Conceptualization, Data curation, Formal Analysis, Funding acquisition, Investigation, Methodology, Project administration, Resources, Software, Supervision, Validation, Visualization, Writing–original draft, Writing–review and editing.

Funding

The author(s) declare that financial support was received for the research, authorship, and/or publication of this article. Authors are thankful to the Faculty of Geography and Geology, Department of Geography, University "Alexandru Ioan Cuza" of Iași, Romania, for financial support.

Acknowledgments

The authors wish to extend their gratitude to the staff of the Romanian Waters Agency Bucharest–Siret Water Administration Bacau, with special appreciation to Gianina Maria Cojoc, a hydrologist at the latter agency, for generously providing the hydrological and climatic data utilized in this study. All data processing was conducted at the Geoarchaeology Laboratory of the Institute for Interdisciplinary Research, Science Research Department, University "Alexandru Ioan Cuza" of Iași (UAIC), Romania. Last but not least, our sincere thanks are extended to all the reviewers whose invaluable feedback significantly contributed to the improvement of the manuscript.

Conflict of interest

The authors declare that the research was conducted in the absence of any commercial or financial relationships that could be construed as a potential conflict of interest.

Publisher's note

All claims expressed in this article are solely those of the authors and do not necessarily represent those of their affiliated organizations, or those of the publisher, the editors and the reviewers. Any product that may be evaluated in this article, or claim that may be made by its manufacturer, is not guaranteed or endorsed by the publisher.

Supplementary material

The Supplementary Material for this article can be found online at: https://www.frontiersin.org/articles/10.3389/feart.2024.1403411/full#supplementary-material

References

Apostol, L. (2004). *Clima subcarpatilor moldovei. (In Romanian), 439*. Editura Universitatii Suceava.

Belayouni, H., Di Staso, A., Guerrera, F., Martín, M., Miclăuş, C., Serrano, F., et al. (2009). Stratigraphic and geochemical study of the organic-rich black shales in the Tarcău Nappe of the moldavidian domain (carpathian chain, Romania). *Int. J. Earth Sci. Geol. Rundsch* 98, 157–176. doi:10.1007/s00531-007-0226-7

Blanch, X., Eltner, A., Guinau, M., and Abellan, A. (2021). Multi-epoch and multi-imagery (MEMI) photogrammetric Workflow for enhanced change detection using time-lapse cameras. *Remote Sens.* 13 (8), 1460. doi:10.3390/rs13081460

Blanch, X., Guinau, M., Eltner, A., and Abellan, A. (2024). A cost-effective image-based system for 3D geomorphic monitoring: an application to rockfalls. *Geomorphology* 449, 109065. doi:10.1016/j.geomorph.2024.109065

Brustur, T., Grinea, D., Briceag, A., and Melinte-Dobrinescu, M.-C. (2019). First record of the upper Eocene amber from central eastern Carpathians (Iapa Valley, neamt county, Romania). *Geo-Eco-Marina* 21 (23), 25–36. doi:10.5281/zenodo.2561003

Bull, J. M., Miller, H., Gravley, D. M., Costello, D., Hikuroa, D. C. H., and Dix, J. K. (2010). Assessing debris flows using LIDAR differencing: 18 May 2005 Matata event, New Zealand. *Geomorphology* 124 (1), 75–84. doi:10.1016/j.geomorph.2010.08.011

Cao, Z., Yue, Z., and Pender, G. (2011a). Landslide dam failure and flood hydraulics. Part I: experimental investigation. *Nat. Hazards* 59, 1003–1019. doi:10.1007/s11069-011-9814-8

Cao, Z., Yue, Z., and Pender, G. (2011b). Landslide dam failure and flood hydraulics. Part II: coupled mathematical modelling. *Na.t Hazards* 59, 1021–1045. doi:10.1007/s11069-011-9815-7

Cheval, S., Birsan, M. V., and Dumitrescu, A. (2014). Climate variability in the carpathian mountains region over 1961–2010. *Glob. Planet. Change* 118, 85–96. doi:10.1016/j.gloplacha.2014.04.005

Chien-Yuan, C., Lien-Kuang, C., Fan-Chieh, Y., Sheng-Chi, L., Yu-Ching, L., Chou-Lung, L., et al. (2008). Characteristics analysis for the flash flood-induced debris flows. *Nat. Hazards* 47, 245–261. doi:10.1007/s11069-008-9217-7

Ciornei, P. (1959). Observații asupra alunecărilor de teren și formării unui nou lac de baraj natural în Maramureș. *Nat. Geogr.* 2, 20–28.

Cojoc, G. M., Romanescu, G., and Tirnovan, A. (2015). Exceptional floods on a developed river: case study for the Bistrita River from the Eastern Carpathians (Romania). *Nat. Hazards* 77, 1421–1451. doi:10.1007/s11069-014-1439-2

Colomina, I., and Molina, P. (2014). Unmanned aerial systems for photogrammetry and remote sensing: a review. *ISPRS J. photogrammetry remote Sens.* 92, 79–97. doi:10.1016/j.isprsjprs.2014.02.013

Costa, J. E., and Schuster, R. L. (1988). The formation and failure of natural dams. *Geol. Soc. Am. Bull.* 100 (7), 1054–1068. doi:10.3133/ofr87392

Cruden, D. M., and Varnes, D. J. (1996). "Landslide types and processes," in *Landslides, investigation and mitigation 247* Editors A. C. Turner, and R. L. Schuster (Transportation Research Board, National Research Council, National Academy Press, Special Report), 36–75.

Dai, F. C., Lee, C. F., Deng, J. H., and Tham, L. G. (2005). The 1786 earthquake-triggered landslide dam and subsequent dam-break flood on the Dadu River, southwestern China. *Geomorphology* 65 (3-4), 205–221. doi:10.1016/j.geomorph.2004.08.011

Decei, P. (1981). *Lacuri de munte (Drumetie si pescuit)*. Bucharest: Editura Sport-Turism.

De Falco, M., Forte, G., Marino, E., Massaro, L., and Santo, A. (2023). UAV and field survey observations on the november 26th 2022 celario flow-slide, ischia island (southern Italy). *J. Maps* 19 (1), 2261484. doi:10.1080/17445647.2023.2261484

De Long, S. B., Prentice, C. S., Hilley, G. E., and Ebert, Y. (2012). Multitemporal ALSM change detection, sediment delivery, and process mapping at an active earthflow. *Earth Surf. Process. Landforms* 37, 262–272. doi:10.1002/esp.2234

Diffenbaugh, N. S., and Field, C. (2013). Changes in ecologically critical terrestrial climate conditions. *Science* 341 (6145), 486–492. doi:10.1126/science.1237123

Eltner, A., Bressan, P. O., Akiyama, T., Gonçalves, W. N., and Marcato Junior, J. (2021). Using deep learning for automatic water stage measurements. *Water Resour. Res.* 57 (3), e2020WR027608. doi:10.1029/2020WR027608

Evans, S. G. (2006). The formation and failure of landslide dams: an approach to risk assessment. *Ital. J. Eng. Geol. Environ.* 1, 15–20. doi:10.4408/IJEGE.2006-01.S-02

Fan, X., Dufresne, A., Subramanian, S. S., Strom, A., Hermanns, R., Stefanelli, C. T., et al. (2020). The formation and impact of landslide dams – state of the art. *Earth-Science Rev.* 203, 103116. doi:10.1016/j.earscirev.2020.103116

Fang, K., Dong, A., Tang, H., An, P., Wang, Q., Jia, S., et al. (2024). Development of an easy-assembly and low-cost multismartphone photogrammetric monitoring system for rock slope hazards. *Int. J. Rock Mech. Min. Sci.* 174, 105655. doi:10.1016/j.ijrmms.2024.105655

Frank, F., Huggel, C., McArdell, B. W., and Vieli, A. (2019). Landslides and increased debris-flow activity: a systematic comparison of six catchments in Switzerland. *Earth Surf. Proc. Land* 44 (3), 699–712. doi:10.1002/esp.4524

Gariano, S. L., and Guzzetti, F. (2016). Landslides in a changing climate. *Earth-Science Rev.* 162, 227–252. doi:10.1016/j.earscirev.2016.08.011

Grasu, C., Catană, C., and Grinea, D. (1988). *Carpahian flysch. Petrography and economic comments. Tehnică, București (in Romanian)*, 1–208.

Guerrera, F., Martin Martin, M., Martin-Perez, A. J., Martin-Rojas, I., Miclaus, C., and Serrano, F. (2012). Tectonic control on the sedimentary record of the central moldavidian basin (eastern Carpathians, Romania). *Geol. Carpathica* 63 (6), 463–479. doi:10.2478/v10096-012-0036-0

Hungr, O., Leroueil, S., and Picarelli, L. (2014). The Varnes classification of landslide types, an update. *Landslides* 11 (2), 167–194. doi:10.1007/s10346-013-0436-y

Hürlimann, M., Coviello, V., Bel, C., Guo, X., Berti, M., Graf, C., et al. (2019). Debris-flow monitoring and warning: review and examples. *Earth-Science Rev.* 199, 102981. doi:10.1016/j.earscirev.2019.102981

Ichim, I., and Rădoane, M. (1996). Geomorphological processes with high recurrence interval in the flysch mountains area (in Romanian). *St. și Cerc., Muz. Șt. Nat. Piatra Neamț* 8, 15–24.

Ilinca, V. (2014). Characteristics of debris flows from the lower part of the Lotru River basin (South Carpathians, Romania). *Landslides* 11, 505–512. doi:10.1007/s10346-014-0489-6

Ilinca, V., and Gheuca, I. (2011). The red lake landslide (ucigașu mountain, Romania). *Carpathian J. Earth Environ. Sci.* 6 (1), 263–272.

Iverson, R. M., Reid, M. E., and LaHusen, R. G. (1997). Debris-flow mobilization from landslides. *Annu. Rev. Earth Planet. Sci.* 25 (1), 85–138. doi:10.1146/annurev.earth.25.1.85

Jaboyedoff, M., Oppikofer, T., Abellán, A., Derron, M.-H., Loye, A., Metzger, R., et al. (2012). Use of LIDAR in landslide investigations: a review. *Nat. Hazards* 61, 5–28. doi:10.1007/s11069-010-9634-2

Jung, K., Shin, J.-Y., and Park, D. (2019). A new approach for river network classification based on the beta distribution of tributary junction angles. *J. Hydrol.* 572, 66–74. doi:10.1016/j.jhydrol.2019.02.041

Kahn, M. E. (2005). The death toll from natural disasters: the role of income, geography, and institutions. *Rev. Econ. Statistics* 87 (2), 271–284. doi:10.1162/0034653053970339

Khasanov, K. (2020). Evaluation of ASTER DEM and SRTM DEM data for determining the area and volume of the water reservoir. *IOP Conf. Ser. Mater. Sci. Eng.* 883, 012063. doi:10.1088/1757-899X/883/1/012063

Korup, O. (2005). Geomorphic imprint of landslides on alpine river systems, southwest New Zealand. *Earth Surf. Process. Landforms* 30 (7), 783–800. doi:10.1002/esp.1171

Lesenciuc, C.-D., Juravle, D. T., Secu, C. V., Nicu, I. C., and Breabăn, I. G. (2017). Using old landslide-dammed llakes to assess sediment delivery rates in small catchments – case study: iezer Lake from the Romanian Carpathians. *Carpathian J. Earth Environ. Sci.* 12 (2), 499–512.

Marchi, L. (2017). "Linking debris flows and landslides to large floods in gravel-bed rivers," in *Gravel-bed rivers: processes and disasters* Editors D. Tsutsumi, and J. B. Laronne (Wiley), 467–495. doi:10.1002/9781118971437.ch17

Miclăuș, C., Loiacono, F., Puglisi, D., and Baciu, D. (2009). Eocene-oligocene sedimentation in the external areas of the moldavide basin (marginal folds Nappe, eastern Carpathians, Romania): sedimentological, paleontological and petrographic approaches. *Geol. Carpathica* 60 (5), 397–417. doi:10.2478/v10096-009-0029-9

Mihu-Pintilie, A. (2018a). "Natural dam lakes and their status within limnological and geographical studies," in *Natural dam lake cuejdel in the stânișoarei mountains, eastern Carpathians 234* Editor A. Mihu-Pintilie (Cham: Springer). doi:10.1007/978-3-319-77213-4_2

Mihu-Pintilie, A. (2018b). "Genesis of the cuejdel Lake and the evolution of the morphometric and morpho-bathymetric parameters," in *Natural dam lake cuejdel in the stânișoarei mountains, eastern Carpathians 234* Editor A. Mihu-Pintilie (Cham: Springer). doi:10.1007/978-3-319-77213-4_5

Mihu-Pintilie, A., Asăndulesei, A., Nicu, I. C., Stoleriu, C. C., and Romanescu, G. (2016). Using GPR for assessing the volume of sediments from the largest natural dam lake of the Eastern Carpathians: cuejdel Lake, Romania. *Environ. Earth Sci.* 75 (8), 710. doi:10.1007/s12665-016-5537-1

Mihu-Pintilie, A., and Dufresne, A. (2023). "Landslide dams in Europe – distribution, data gaps, and further research," in EGU General Assembly 2023 EGU23-5083, Vienna, Austria, 24–28 Apr 2023.

Mihu-Pintilie, A., Paiu, M., Breabăn, I. G., and Romanescu, G. (2014a). Status of water quality in cuejdi hydrographic basin from eastern carpathian, Romania. *Int. Multidiscip. Sci. GeoConference-SGEM* 14, 639–646. doi:10.5593/SGEM2014/B31/S12.083

Mihu-Pintilie, A., Romanescu, G., and Stoleriu, C. C. (2014b). The seasonal changes of the temperature, pH and dissolved oxigen in the Cuejdel Lake, Romania. *Carpathian J. Earth Environ. Sci.* 9, 113–123.

Mîndrescu, M., Cristea, A. I., Hutchinson, S. M., Florescu, G., and Feurdean, A. (2013). Interdisciplinary investigations of the first reported laminated lacustrine sediments in Romania. *Quat. Int.* 293, 219–230. doi:10.1016/j.quaint.2012.08.2105

Năstase, Gh. I. (1949). Un lac necunoscut: lacul Bolătău din comuna Dărmănești, județul Bacău. *Rev. Stiintifica V. Adamachi* 35 (1-2), 23–30.

Neugirg, F., Stark, M., Kaiser, A., Vlacilova, M., Della Seta, M., Vergari, F., et al. (2016). Erosion processes in calanchi in the Upper Orcia Valley, Southern Tuscany, Italy based on multitemporal high-resolution terrestrial LiDAR and UAV surveys. *Geomorphology* 269, 8–22. doi:10.1016/j.geomorph.2016.06.027

Neumayer, E., and Barthel, F. (2011). Normalizing economic loss from natural disasters: a global analysis. *Glob. Environ. Change* 21 (1), 13–24. doi:10.1016/j.gloenvcha.2010.10.004

Ochtyra, A., Marcinkowska-Ochtyra, A., and Raczko, E. (2020). Threshold- and trend-based vegetation change monitoring algorithm based on the inter-annual multi-temporal normalized difference moisture index series: a case study of the Tatra Mountains. *Remote Sens. Environ.* 249, 112026. doi:10.1016/j.rse.2020.112026

Ortiz-Giraldo, L., Botero, B. A., and Vega, J. (2023). An integral assessment of landslide dams generated by the occurrence of rainfall-induced landslide and debris flow hazard chain. *Front. Earth Sci.* 11, 1157881. doi:10.3389/feart.2023.1157881

Petley, D. (2012). Global patterns of loss of life from landslides. *Geology* 40 (10), 927–930. doi:10.1130/G33217.1

Pop, G. P. (1970). Lacul Dătășeni – aspecte morfo-hidrografice. *Lucr. Colocviului Limnol. Fiz.* 1, 67–72.

Pop, O. T., Germain, D., Meseșan, F., Gavrilă, I. G., Alexe, M., Buzilă, L., et al. (2019). Dendrogeomorphic assessment and sediment transfer of natural vs. mining-induced debris-flow activity in Călimani Mountains, Eastern Carpathians, Romania. *Geomorphology* 327, 188–200. doi:10.1016/j.geomorph.2018.10.028

Pop, O. T., Ilinca, V., Anghel, T., Gavrilă, I. G., and Popescu, R. (2017). "Debris flows in călimani mountains and lotrului valley," in *Landform dynamics and evolution in Romania* Editors M. Radoane, and A. Vespremeanu-Stroe (Cham: Springer Geography. Springer). doi:10.1007/978-3-319-32589-7_14

Romanescu, G., Cimpianu, C. I., Mihu-Pintilie, A., and Stoleriu, C. C. (2017). Historic flood events in NE Romania (post-1990). *J. Maps* 13 (2), 787–798. doi:10.1080/17445647.2017.1383944

Romanescu, G., Mihu-Pintilie, A., and Stoleriu, C. C. (2018b). "The Pond of God: the largest landslide-dammed lake in Romania," in *Proocedings of international conference water resources and wetlands* Editors P. Gastescu, W.Jr. Lewis, and P. Bretcan 4 (Transversal Publishing House), 86–94.

Romanescu, G., Mihu-Pintilie, A., Stoleriu, C. C., Carboni, D., Paveluc, L. E., and Cimpianu, C. I. (2018a). A comparative analysis of exceptional flood events in the context of heavy rains in the summer of 2010: Siret basin (NE Romania) case study. *Water* 10, 216. doi:10.3390/w10020216

Romanescu, G., Stoleriu, C. C., and Enea, A. (2013). "Definition of lakes and their position in the Romanian territory," in *Limnology of the red lake, Romania* (Dordrecht: Springer). doi:10.1007/978-94-007-6757-7_1

Santangelo, N., Forte, G., De Falco, M., Chirico, G. B., and Santo, A. (2021). New insights on rainfall triggering flow-like landslides and flash floods in Campania (Southern Italy). *Landslides* 18, 2923–2933. doi:10.1007/s10346-021-01667-9

Santo, A., Di Crescenzo, G., Forte, G., Papa, R., Pirone, M., and Urciuoli, G. (2018). Flow-type landslides in pyroclastic soils on flysch bedrock in southern Italy: the Bosco de' Preti case study. *Landslides* 15, 63–82. doi:10.1007/s10346-017-0854-3

Sassa, K., and Wang, G. (2005). "Mechanism of landslide-triggered debris flows: liquefaction phenomena due to the undrained loading of torrent deposits," in *Debris-flow hazards and related phenomena. Springer praxis books* (Berlin, Heidelberg: Springer). doi:10.1007/3-540-27129-5_5

Scheip, C., and Wegmann, K. (2022). Insights on the growth and mobility of debris flows from repeat high-resolution lidar. *Landslides* 19, 1297–1319. doi:10.1007/s10346-022-01862-2

Sepúlveda, S. A., and Padilla, C. (2008). Rain-induced debris and mudflow triggering factors assessment in the Santiago cordilleran foothills, Central Chile. *Nat. Hazards* 47, 201–215. doi:10.1007/s11069-007-9210-6

Serban, G., Hognogi, G., and Man, O. (2012). "New elements concerning the morphology and the morphometry of the sliding lake of Căian (Bistrița-Năsăud County)," in *Proocedings of international conference water resources and wetlands* Editors P. Gastescu, W.Jr. Lewis, and P. Bretcan 2 (Transversal Publishing House), 87–93.

Stoleriu, C. C., Stoleriu, O., and Mihu-Pintilie, A. (2014). Scientific and tourist value of natural dam lakes in the carpathian mountains (Romania). Case study: red, cuejdel and iezerul sadovei lakes. *SGEM Proc. 14th Int. Multidiscip. Sci. Geoconferences–Ecology Environ. Prot.* 14 (2), 625–632.

Tannant, D. D., and Skermer, N. (2013). Mud and debris flows and associated earth dam failures in the Okanagan region of British Columbia. *Can. Geotech. J.* 50, 820–833. doi:10.1139/cgj-2012-0206

Tichavský, R., Fabiánová, A., Koutroulis, A., Spálovský, V., and Vala, O. (2023). Recent debris-flow activity on the 1913 Tsivlos landslide body (Northern Peloponnese; Greece). *CATENA* 231, 107318. doi:10.1016/j.catena.2023.107318

Tiranti, D., Crema, S., Cavalli, M., and Deangeli, C. (2018). An integrated study to evaluate debris flow hazard in alpine environment. *Front. Earth Sci.* 6 (60). doi:10.3389/feart.2018.00060

Tövissi, I. (1964). Câteva caractere morfo-hidrografice ale Lacului Rat de la Porumbenii Mari (raionul Odorhei). Studia Universitatis Babeș-Bolyai. *Ser. Geogr. Fasc.* 1, 107–112.

Vădean, R., Arghiuș, V., and Pop, O. (2015). Dendrogeomorphic reconstruction of past debris-flood activity along a torrential channel: an example from Negoiul basin (Apuseni Mountains, Romanian Carpathians). *Z. für Geomorphol.* 59 (3), 319–335. doi:10.1127/zfg/2014/0156

Yang, W., Wan, F., Ma, S., Qu, J., Zhang, C., and Tang, H. (2023). Hazard assessment and formation mechanism of debris flow outbursts in a small watershed of the Linxia Basin. *Front. Earth Sci.* 10, 994593. doi:10.3389/feart.2022.994593

Yang, Z., Wang, L., Qiao, J., Uchimura, T., and Wang, L. (2020). Application and verification of a multivariate real-time early warning method for rainfall-induced landslides: implication for evolution of landslide-generated debris flows. *Landslides* 17, 2409–2419. doi:10.1007/s10346-020-01402-w

Yermolaev, O., Usmanov, B., Gafurov, A., Poesen, J., Vedeneeva, E., Lisetskii, F., et al. (2021). Assessment of shoreline transformation rates and landslide monitoring on the bank of Kuibyshev Reservoir (Russia) using multi-source data. *Remote Sens.* 13 (21), 4214. doi:10.3390/rs13214214

Zhao, T., Zhou, G. G. D., Sun, Q., Crosta, G. B., and Song, D. (2022). Slope erosion induced by surges of debris flow: insights from field experiments. *Landslides* 19, 2367–2377. doi:10.1007/s10346-022-01914-7

Glossary

a.s.l.	Above Sea Level
ASTER	Advanced Spaceborne Thermal Emission and Reflection Radiometer
DEM	Digital Elevation Model
DTM	Digital Terrain Model
DOD	DEM of Difference
GCD	Geomorphic Change Detection
GIS	Geographic Information System
GDS	Ground Sampling Distance
GPS	Global Positioning System
LDF	Landslide triggered debris flow
NDMI	Normalized Difference Moisture Index
PCP	Projection Center Point coordinates
RTK	Real-Time Kinematic
SRTM	Shuttle Radar Topography Mission
UAV	Unmanned Aerial Vehicle